frontiers | Frontiers in Astronomy and Space Sciences

TYPE Review
PUBLISHED 11 August 2023
DOI 10.3389/fspas.2023.1195654

OPEN ACCESS

EDITED BY
Joseph E. Borovsky,
Space Science Institute (SSI), United States

REVIEWED BY
Caitriona Jackman,
Dublin Institute for Advanced Studies (DIAS), Ireland
Peter H. Yoon,
University of Maryland, College Park, United States
Colin Forsyth,
University College London, United Kingdom

*CORRESPONDENCE
James LaBelle,
james.w.labelle@dartmouth.edu

RECEIVED 28 March 2023
ACCEPTED 24 July 2023
PUBLISHED 11 August 2023

CITATION
LaBelle J (2023), Radio emissions of auroral origin observable at ground level: outstanding problems.
Front. Astron. Space Sci. 10:1195654.
doi: 10.3389/fspas.2023.1195654

Radio emissions of auroral origin observable at ground level: outstanding problems

James LaBelle*

Department of Physics and Astronomy, Dartmouth College, Hanover, NH, United States

Auroral radio emissions are of intrinsic interest as part of the Earth's environment but also provide remote sensing of ionospheric conditions and processes and a laboratory for emission processes applicable to a wide range of space and astrophysical plasmas. At VLF and above, four broad classes of radio emissions occur. All have been observed with ground-based and, in some cases to a lesser degree, with space-based instruments. Related to each type of radio emission, many experimental and theoretical challenges remain, for example: explanations of frequency and time structure, relations to auroral substorms or current systems, and application to remote sensing of the auroral ionosphere. In some cases, basic parameters such as source heights or generation mechanisms are uncertain. Emerging technological advances such as cubesat fleets, ultra-large capacity disk drives, and software defined radio show promise for developing better understanding of auroral radio emissions.

KEYWORDS

radio emissions, aurora, plasma waves, ionospheric propagation, auroral kilometric radiation, auroral hiss, substorms

1 Introduction

There are four broad classifications of radio emissions of terrestrial auroral origin observable at ground level in the VLF band and at higher frequencies: 1) auroral cyclotron harmonic emissions, narrowband and occurring at cyclotron harmonics; 2) auroral medium frequency burst, broadband at 1.3–5.0 MHz; 3) auroral hiss, broadband below 1.3 MHz; and 4) leaked auroral kilometric radiation at hundreds of kHz. There are sub-types of each of these. Besides being of intrinsic interest as part of Earth's environment, plasma waves, radiation, and associated wave-particle interactions sometimes significantly affect macroscopic structure or processes, as happens, for example, in Earth's radiation belts. They also provide tools for remotely sensing ionospheric conditions or processes from ground level; determination of magnetospheric density structure using atmospheric whistlers (Carpenter, 1963) is a famous example, as is the use of escaping auroral kilometric radiation to remotely detect the altitude extent of the auroral acceleration region (Morioka et al., 2007; Morioka et al., 2014, and references therein). Another motivation to understand auroral radio emissions results from their similarity to planetary, solar, and astrophysical radio emissions (review by Zarka, 1998), which implies that they serve as a local laboratory for investigating widely applicable plasma radio emission processes. For example, Yoon et al. (2006) points out that the generation and structuring mechanism of auroral cyclotron emission is nearly identical to that for planetary continuum radiation. Several reviews cover radio emissions of auroral origin at VLF (e.g., Sazhin et al., 1993;

Sonwalkar et al., 1995) and LF/MF/HF (Ellyett, 1969; LaBelle, 1989; LaBelle and Treumann, 2002). This review focusses on current outstanding problems in this sub-field of space physics.

2 Auroral cyclotron harmonic emissions

Auroral cyclotron harmonic emissions have been studied intensely both from ground-level and from above the ionosphere. The phenomenon was first observed with the ISIS satellites topside sounder receivers and called "2-MHz" and "4-MHz" noise due to occurrence at those frequencies (James et al., 1974; Benson and Wong, 1987). A similar phenomenon referred to as "terrestrial hectametric radiation" (THR) was observed with the Akebono satellite (Oya et al., 1985; Oya et al., 1990). In these original papers, THR referred to a broadband LO-mode emission above the local plasma frequency, but Sato et al. (2010) report examples also called THR but concentrated near 2- and 4-MHz that closely resemble the earlier ISIS satellite observations. Bale. (1999) reports a single remote detection of waves near 1.8- and 4.4-MHz resembling cyclotron harmonic radiation observed near $6R_E$ (38,000 km) with the WIND spacecraft. Cyclotron harmonic radiation has also been observed at ionospheric altitudes from sounding rockets (e.g., Morioka et al., 1988; Dombrowski et al., 2016). Ground-level cyclotron harmonic emissions were first observed near 3 MHz, associated with $2f_{ce}$ (Kellogg and Monson, 1979), and subsequently at higher frequencies associated with $3f_{ce}$ (Weatherwax et al., 1993), $4f_{ce}$ (Sato et al., 2012), and $5f_{ce}$ (LaBelle, 2011). Figure 1 shows a rare example of simultaneous $2f_{ce}$, $3f_{ce}$, and $4f_{ce}$ emissions observed at Toolik Lake, Alaska. Usually only one or at most two such emissions are observed at a time.

At ground level, cyclotron harmonic emissions are most favorably observed at stations a few degrees poleward of the auroral zone due to auroral absorption affecting observations under the aurora. Along the "Churchill meridian" in the northern hemisphere, occurrence rate peaks near 75° magnetic latitude where emissions occur approximately 5% of favorable local times and season (Hughes and LaBelle, 1998). Sato et al. (2015) report a much lower occurrence rate from Longyearbyen (magnetic latitude 75.4) of 0.19% averaged over all local times and seasons, the discrepancy attributed to differences in methodology. The occurrence rate at Hussafjell, Iceland (magnetic latitude 65.3°) is much lower, consistent with the decreased occurrence at auroral latitudes reported by Hughes and LaBelle. (1998) and the absence of events at an auroral latitude (Cleary, Alaska) reported by Kellogg and Monson. (1984). Occurrence rates in space may be considerably higher. ISIS-1 detected "2-MHz noise," equivalent to $2f_{ce}$ harmonic emissions, on 10%–20% of ionograms during two 3-4-day magnetically disturbed intervals (James et al., 1974; Benson and Wong, 1987). Sato et al. (2015) report a 0.46% overall occurrence rate of THR emissions in the Akebono data set, considerably higher than the comparable ground-based value determined with similar methodology (0.19% at Longyearbyen).

The radiance of cyclotron harmonic emissions at ground level has been reported as a few times 10^{-18} W/m^{2}Hz (Weatherwax et al., 1993; Kellogg and Monson, 1979), although they range from 1-2 orders of magnitude larger to as low as 10^{-19} W/m^{2}Hz (Sato et al., 2008) which is close to the observation threshold set by the galactic background at these frequencies. In space, James et al. (1974) report typical intensities of "2-MHz noise" and "4-MHz noise" ranging from 25–40 dB above the galactic background level, implying 10^{-18} to 10^{-17} W/m^{2}Hz, with "4-MHz" noise about 10 dB weaker in general. Their measurements are of storm-time events above 1,000 km altitude. Benson and Wong. (1987) analyze data from the same satellite near perigee (500 km), stating that the "2-MHz" signals are about 7-dB below the 0.01 mV/m integrated field strength, corresponding to about 10^{-17} W/m^{2}Hz. Sato et al. (2015) show spectrograms of 2- and 4-MHz THR with radiances exceeding 3×10^{-16} to 3×10^{-15} V^2/m^{2}Hz (10^{-18} to 10^{-17} W/m^{2}Hz).

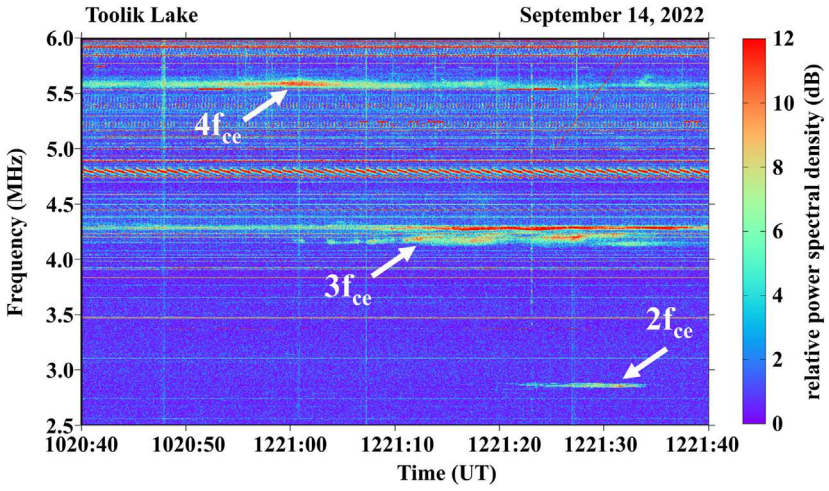

FIGURE 1
An unusual case of simultaneous auroral cyclotron harmonic emissions near three different harmonics of the electron cyclotron frequency, detected with a 10-m^2 loop antenna and digital receiving system operated at Toolik Lake, Alaska (68.63 N, 149.61 W, geomagnetic latitude 68.7°).

The generation mechanism of these emissions starts with upper hybrid waves generated at the "double resonance" condition $f = f_{uh} = Nf_{ce}$ for $N = 1,2,3\ldots$, followed by mode conversion to LO mode radiation (James et al., 1974; Kaufmann, 1980; Gough and Urban, 1983; Yoon et al., 1998a). Several studies showed that Dory-Guest-Harris (DGH), ring, or loss cone distributions lead to large growth rates of the cyclotron maser instability near the double resonance condition (e.g., Figure 8 of Benson and Wong, 1987; Figures 2, 3 of Yoon et al., 1998a). Yoon et al. (1998b) showed how the resulting waves, primarily perpendicular to B, could be refracted in density gradients to achieve linear conversion to LO-mode, though subsequent studies of fine structure of the emissions suggest that small-scale density irregularities play a role in the conversion, which may occur via wave-wave interaction followed by scattering on density irregularities as suggested by James et al. (1974). The double resonance condition occurs both on the topside, explaining most of the satellite and rocket observations, and on the bottomside, explaining most of the ground based observations. Hughes et al. (2001) show evidence of ground-level reception of signals from both the bottomside and topside locations.

Numerous observations support this mechanism, starting with ray-tracing demonstrating that sources illuminating the satellite path over which ISIS detected the "2-MHz" emissions are located where $f = f_{uh} = 2f_{ce}$ (James et al., 1974). Hughes and LaBelle. (2001a) performed a similar experiment at ground-level using interferometry to determine directions of arrival of $2f_{ce}$ emissions and, through ray-tracing in two-dimensional ionospheric structure simultaneously measured with a scanning incoherent scatter radar, determining that these originated where $f = f_{uh} = 2f_{ce}$. Sato et al. (2010) observe a strong enhancement in intensity of $2f_{ce}$ emissions when the Akebono satellite encountered them where the "double resonance" condition holds, with a $1/r^2$ intensity dependence decreasing as the satellite moved away from that location, suggesting that the source of the emissions is where $f = f_{uh} = 2f_{ce}$. Hughes and LaBelle. (1998) showed that frequencies of the $2f_{ce}$ ($4f_{ce}$) emissions increase with magnetic latitude of the observing station as expected if it were associated with cyclotron resonance near 275 (375) km altitude. The ground-level emissions were observed to be polarized appropriate for the LO-mode as predicted by the theory (e.g., Shepherd et al., 1997; Sato et al., 2008). LaBelle and Dundek. (2015) showed that occurrence of higher harmonics required successively higher solar zenith angles, consistent with higher ionospheric density needed to achieve the "double resonance" condition at higher harmonics, and consistent with observations that the highest harmonic $4f_{ce}$ and $5f_{ce}$ emissions occur in daylit ionosphere (Sato et al., 2012; LaBelle, 2012). The observations of LaBelle and Dundek. (2015) also highlight that typically only the highest, or sometimes the highest two, harmonic emissions allowed by the density profile are observed; rarely do multiple harmonics occur simultaneously as shown in Figure 1. Sato et al. (2015) point out that although adiabatic evolution of the auroral electron beam suggests steeper $df/dv_\perp$ at lower altitudes, reduction of $df/dv_\perp$ through wave-particle interactions with higher altitude electrostatic waves may favor excitation at higher altitudes (and hence higher harmonics). This effect may also explain differences in satellite and ground-level observations of cyclotron harmonic emissions (Sato et al., 2015). Detailed modeling of the evolving distribution function may reveal why particular harmonics are favored.

The earliest observations suggested that at least a subset of "4-MHz" emissions, associated with $4f_{ce}$, arise from a different mechanism, possibly second harmonic generation of waves generated at the $f = f_{uh} = 2f_{ce}$ matching condition (James et al., 1974). Sato et al., (2010), using Akebono satellite data, observed $4f_{ce}$ emissions with right-hand polarization opposite to that expected for mode-converted upper hybrid waves, occurring in coincidence with left-polarized $2f_{ce}$ emissions of exactly half their frequency. They found ten examples following this identical pattern in the Akebono satellite data and suggested that nonlinear coalescence of upper hybrid waves generated at the $2f_{ce}$ matching condition is responsible for the observed $4f_{ce}$ waves. Sato et al. (2015) reported two cases of right-hand polarization among eleven $4f_{ce}$ emissions measured at ground level in Iceland; those two also stood out as being observed in darkness when the density is not high enough to support direct emission of $4f_{ce}$. LaBelle and Chen. (2016) systematically analyzed all $4f_{ce}$ emissions observed during a ten-month period at Sondrestrom, Greenland, finding that the vast majority of emissions were left-hand polarized and observed under daylit conditions, while a small number were right-hand polarized and observed in darkness. These studies suggest that while most $4f_{ce}$ emissions arise from the usual mechanism, mode-conversion of waves generated at the double resonance producing LO-mode waves and requiring relatively high densities and daylit conditions, occasional $4f_{ce}$ emissions result from harmonic generation of upper hybrid waves at the $2f_{ce}$ double resonance which occurs favorably in lower densities/darkness conditions. Theoretical work by Yoon et al., (2016) confirmed the expectation of right-hand polarization for the coalescence mechanism (Earlier work by Willes et al., (1998) considered coalescence as a potential source of cyclotron harmonic emissions).

High-resolution measurements show that cyclotron harmonic emissions exhibit both temporal and frequency fine structure. They consist of a multitude of narrow-band structures with complex frequency-time variations (LaBelle et al., 1995) having bandwidths <1 kHz and as narrow as a few Hz, with an astonishing range of characteristics such as multiplet structures (Shepherd et al., 1998). Yoon et al. (2000) showed that in the presence of density irregularities of scale size comparable to their wavelength, the causative upper hybrid waves generated at the double-resonance condition occur in patterns of discrete frequencies, resulting in mode conversion radiation mirroring those discrete features. A rocket-borne wave receiver serendipitously encountering the double-resonance source region detected upper hybrid waves with structure qualitatively matching the theoretical predictions (Samara et al., 2004). Ye et al., (2007) found that a significant subset of observed ground-level cyclotron harmonic fine structure could also be matched qualitatively to the theory, but that quantitative matching of either the rocket or ground-based data had ambiguities, probably because of limitations of the theory such as cylindrical symmetry which may seldom apply to ionospheric irregularities, and perfectly perpendicular wave vectors which is also not realistic. Yoon et al. (2006) highlight the analogy between the cyclotron harmonic waves and terrestrial continuum radiation which may be structured by a similar mechanism.

In addition to frequency fine structure, cyclotron harmonic radiation exhibits temporal fine structure such as modulations at tens of Hz dubbed "flickering auroral roar" because its time scale

matches that of flickering aurora (Hughes and LaBelle, 2001b). Based on time duration, flickering characterizes only a few percent of $2f_{ce}$ cyclotron harmonic emissions (Ye et al., 2006). This low occurrence rate could be due to the broad beam antennas used in the measurements which tend to wash out the phenomenon if it occurs in small patches similar to optical flickering aurora. The flickering tends to affect the lowest radio emission frequencies, a characteristic shown by Weatherwax et al., (2006) to be consistent with generation of flickering aurora through acceleration in ion cyclotron waves (Temerin et al., 1986; 1993).

The outstanding question concerning auroral cyclotron harmonic emissions is explaining the wide range of fine structure features that characterize the phenomenon. A significant subset of these are at least qualitatively consistent with predicted discretization of the causative upper hybrid wave modes due to density irregularities in the source region (Yoon et al., 2000). This mechanism predicts multiplet structures often observed. Some observations are in remarkably good qualitative agreement with the theory, such as rocket observations of the causative upper hybrid waves (though not the electromagnetic emission) showing the predicted pattern of nested multiplet structures with different spacings (Samara et al., 2004). However, attempts to explain this event and a broader set of ground-level observations quantitatively using existing theory assuming cylindrically symmetric density structures give mixed results (Ye et al., 2007). These studies highlight the need to generalize the theory to more realistic non-cylindrically symmetric density structures. Although a significant subset of the emissions consists of multiplet-like structures which may be explained by suitably generalized eigenmode theory, it is not clear that this mechanism can explain the entire range of fine structure features. It remains an open question whether other structuring processes operate, related to wave generation, propagation, or scattering. This problem is fundamental to the nature of mode-conversion radiation which occurs in a wide range of planetary, solar, and astrophysical plasmas, and its solution would enable new methods of remotely sensing auroral ionospheric plasma conditions and processes using cyclotron harmonic emissions and other related types of emissions.

Another open question is the connection between flickering auroral roar (Hughes and LaBelle, 2001b) and the optical flickering aurora. Assuming such a connection holds, the radio phenomenon favors one flickering model over others (Ye et al., 2006; Weatherwax et al., 2006). The challenge is that optical flickering typically comes from relatively small patches in the sky, whereas radio observations have hitherto been broad-beam. Success with radio interferometry applied to cyclotron harmonic emissions raises the possibility of associating direction of arrival of flickering radio emissions with locations of observed optically flickering patches. The phase relation between the radio emission maxima and the maxima in light emission would also provide smoking-gun evidence of an association. Suitable simultaneous optical imaging and radio interferometry are needed to answer this question.

There is ample indirect evidence that nonlinear processes are responsible for a subset of $4f_{ce}$ harmonic roar emissions, such as the anomalous polarization (right-hand) and frequency (lower than normal) of the emissions, their occurrence during nighttime when electron density is usually too low to support the normal mechanism of producing $4f_{ce}$ emissions, and simultaneous observation of $2f_{ce}$ emission at exactly half the frequency (Sato et al., 2010; Sato et al., 2015; LaBelle and Chen, 2016). This impressive array of evidence arose entirely from remote sensing. Stronger proof requires observations of the harmonically related $2f_{ce}$ and $4f_{ce}$ waves in or near the source region to examine the phase relations between them expected if they are components of a wave-wave interaction. This question is worth answering since this phenomenon represents one of relatively few naturally occurring nonlinear plasma phenomena in near-Earth plasma subject to direct observations. Extensive experiments on similar man-made nonlinear phenomena involving active RF heating of the ionosphere may provide a guide for investigations or even be directly informative (Leyser, 2001; Grach et al., 2016).

Propagation in the disturbed auroral ionosphere strongly affects ground-based observations of cyclotron harmonic emissions, as evidenced by their sporadic nature during substorm break-up/onset phase and general absence during recovery phase (e.g., LaBelle et al., 1994). Also, they are generally not observed from sites equatorward of the auroral zone due to ionization caused by diffuse aurora (e.g., Kellogg and Monson, 1984). Better understanding of their prevalence, intensity, latitude distribution, and particularly occurrence in substorm phases beyond the growth phase, requires satellite observations which are unaffected by ionospheric absorption. The Japanese Akebono satellite has provided many observations, including two examples of simultaneous space-based and ground-level observations, although in neither case did ground- and space-based instruments observe exactly the same source (Sato et al., 2016); more commonly emissions were observed only from ground or from spacecraft, even when the spacecraft was above the ground stations. The early ISIS low-Earth-orbit satellites obtained occurrence statistics of large numbers of "2-MHz" and "4-MHz" emissions, identical to what are now known as $2f_{ce}$ and $3f_{ce}$ harmonic emissions (Benson and Wong, 1987). In some cases these were the subject of detailed case studies (James et al., 1974). Occasional space-based observations at greater distances may be associated with auroral cyclotron emissions (e.g., Bale, 1999). However, understanding the behavior of cyclotron harmonic waves during the onset and recovery phases of substorms requires multiple satellite passes during different substorm phases, including direction finding or radio imaging since the spacecraft will not always be in the right place at the right time. Furthermore, simultaneous satellite and ground-based direction-finding measurements, by determining whether the same source is being observed, would inform the interpretation of the intensity of the ground-level signals and provide better estimates of the effective radiative power of the sources.

Another open question about auroral cyclotron harmonic emissions concerns their use for remotely sensing electron density or electron density profiles. Mode-conversion radiation at the double resonance predicts that higher harmonics require higher electron densities, so the mere presence of particular harmonic emissions implies limits on the F-peak density; Weatherwax et al. (2006) provide diagnostic tools based on this idea. Harmonics up to $5f_{ce}$ have been observed; it's an open question whether higher harmonics occur and if not, why not. Burnett and LaBelle. (2020) introduce a more subtle technique for remotely sensing the electron density profile using direction finding, exploiting the requirement that observed emissions originate at known altitudes predicted by

the double-resonance mode-conversion mechanism. This technique was confirmed by comparison with incoherent scatter radar data in two case studies, but its validation requires more theoretical and experimental development. Because the theory predicts the source altitudes and some characteristics of the wave vectors of cyclotron harmonic emissions, direction-finding observations combined with ray-tracing have promise to reveal much information about the electron density profile and structure, especially when more than one harmonic is observed simultaneously, either from space or ground level.

3 Auroral medium frequency burst emissions

Auroral Medium Frequency Burst (MFB) appears in low-resolution spectrograms as a broadband impulsive emission typically spanning a 500–1,500 kHz band within the 1.3–5.0 MHz frequency range. It was first definitively described from ground-based observations of Weatherwax et al. (1994), although earlier observations referred to a burst component of emissions which may have been the same phenomenon or may have been lightning generated sferics which can appear similar (Kellogg and Monson, 1979). In retrospect, Benson and Desch (1991) likely observed a simultaneous MFB and auroral hiss event at Andoya, Norway, in 1989. MFB often occurs at substorm onsets, in association with impulsive auroral hiss, a bay in the H-component of the geomagnetic field, prompt riometer absorption, and auroral brightening (LaBelle et al., 1994; Sato et al., 2008; Bunch et al., 2008), though it sometimes accompanies auroral activations that fall short of substorm onset. In a recent study, Hudson et al. (2022) show that 50% of a large sample of MFB events over a two-year period are associated with substorm onsets in the same geographical sector independently identified by algorithms using a magnetometer database. Bunch et al. (2008), Bunch et al. (2009) used interferometry to show cases of MFB originating at the locations of substorm onsets simultaneously imaged with ground-based all-sky cameras. These data from Toolik Lake, which lies poleward of the aurora most of the time, show that the elevation angle of arrival of MFB increases with time as the substorm arc advances poleward toward the observatory. When the arc moves overhead, the MFB disappears from the ground-level record, presumably because of absorption in the dense ionosphere underneath the substorm arcs. For this reason, MFB at ground level lasts a short time, typically seconds to tens of minutes, preceding substorm onsets or other auroral activations. The poleward motion of MFB in concert with substorm expansion is also observed in data from a meridional chain of observatories, where MFB appears and disappears in succession at more northerly locations [Figure 6 of LaBelle et al., 2005].

It is not known whether MFB continues for a longer time in space after auroral absorption wipes out the ground-level observations. In fact, it is not certain whether MFB has been detected in space at all. The DEMETER spacecraft detected 68 examples of broadband impulsive radiation at 1.5–3.0 MHz resembling MFB during limited intervals when it sampled high-latitudes, in one case in coincidence with MFB observed at ground-level in a near-conjugate observatory (Broughton et al., 2015). The Akebono spacecraft detects broadband noise with a lower cutoff at the local plasma frequency called terrestrial hectametric radiation (THR) (Oya et al., 1985; Oya et al., 1990), though examples shown in the literature do not strongly resemble MFB. Sato et al. (2015) show an example of structured THR spanning 1.2–4.7 MHz which may at least partly represent MF burst although they attribute it to cyclotron harmonic emission from multiple sources. Other spacecraft and rocket experiments also detect structured emissions around the plasma and upper hybrid frequencies (e.g., Beghin et al., 1989; McAdams and LaBelle, 1999) but with no established connection to MFB.

South Pole observations spanning calendar year 2004 show that darkness is required for observing MFB at ground level and that most events occur in a 4-5 h window around midnight MLT, not surprising given their association with substorms; 103 events occur during the half-year of darkness, implying an occurrence rate of 0.57% during favorable magnetic local times and solar zenith angles (LaBelle et al., 2005). Broughton et al. (2015) calculate a similar occurrence rate (0.62%) based on a larger data set (1994-2008 Churchill observations). The Churchill data indicate that about one-third of ground-level MFB have average radiance exceeding 10^{-18} W/m^{2}Hz, which can be taken as a typical value; peak radiance might be one to two orders of magnitude greater. As mentioned above, observations of MFB in space are few and uncertain. MFB-like signals observed with the DEMETER satellite had occurrence rate of 0.76% (Broughton et al., 2015). Broughton et al. (2016) state that the integrated rms amplitude of these waves is 25–100 μV/m, implying $1–5 \times 10^{-18}$ W/m^{2}Hz, but grayscale spectrograms in their paper suggest higher radiances of order 10^{-16} W/m^{2}Hz.

There is evidence that the MFB frequency range is related to the maximum ionospheric electron density. LaBelle et al. (1997) observed in a case study that the MFB frequency jumped higher at the time of a significant increase in density measured with a co-located incoherent scatter radar. LaBelle et al. (2005) show statistically over the course of a year's observations that the maximum frequency of MFB increases with solar zenith angle and therefore with increasing peak ionospheric density. MFB often occurs in bands that roughly span the frequency range between electron gyro-harmonics; Figure 2 shows examples of "low band" MFB (~1.5–2.5 MHz), "high band" MFB (3-4 MHz), and "high-high band" MFB (up to about 5 MHz). When MFB extends across twice the electron gyrofrequency (~2.8 MHz), a null often appears at that frequency as first noted by Weatherwax et al. (1994). The null is typically broad (tens of kHz) but occasionally very narrow (<1 kHz). "Low band" MFB often exhibits an abrupt lower cutoff near 1.4 MHz, which may be associated with either the electron gyrofrequency or ionospheric L-cutoff, and when MFB appears below this cutoff, there is a small gap (Figure 22 of LaBelle and Treumann, 2002; LaBelle, 2018). The MFB above the cutoff has been shown early on to be left-polarized, consistent with LO-mode in the ionosphere (Shepherd et al., 1997). The component below the cutoff has recently been shown to be left-polarized as well (LaBelle, 2018), implying it must also be LO-mode and contradicting speculation that it might be whistler mode.

Early observations showed hints that MFB consists of fast (~milliseconds) variations and fine structure (LaBelle et al., 1997). Fully resolved measurements show that the view of MFB as broadband impulsive emission based on low-resolution

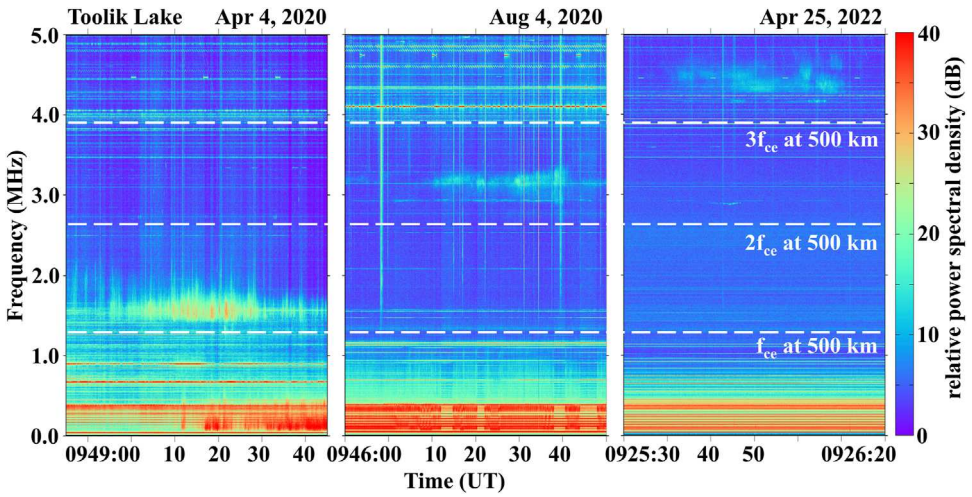

FIGURE 2
Three examples of MFB occurring in (left panel) "low band" (at 1.4–2.2 MHz in this case, roughly between f_{ce} and $2f_{ce}$), (middle panel) "high band" (at 2.8–3.5 MHz, roughly between $2f_{ce}$ and $3f_{ce}$), and (right panel) "high-high-band" (at 4.2–5.0 MHz in this case, roughly between $3f_{ce}$ and $4f_{ce}$). The instrumentation used for these measurements is identical to that used for those shown in Figure 1. For reference, dashed lines indicate the electron cyclotron frequency and its harmonics.

measurements is misleading; MFB consists of superpositions of many short-duration frequency-dispersed features having bandwidths kHz to hundreds of kHz and time durations milliseconds to hundreds of milliseconds (Bunch and LaBelle, 2009). There is a broadband background component which may be consistent with superposition of large numbers of weaker fine structures. A zoo of features occur, including rising, falling, and monochromatic tones, but a common feature, called "backwards seven," consists of a narrowband tone decreasing by tens to hundreds of kHz during tens to hundreds of milliseconds, sometimes initiated by a sharper tone of increasing frequency (Bunch and LaBelle, 2009). LaBelle. (2011) showed that this feature can be produced by a relatively low energy electron beam generating Langmuir waves over a range of heights and therefore densities in the topside ionosphere, followed by mode-conversion to LO-radiation that reaches the ground. Such low-energy parallel electron beams resulting from Alfvénic acceleration characterize the substorm onset arc (e.g., Mende, 2003; Mende et al., 2003). Mode-conversion of topside Langmuir waves could explain a range of fine structure dispersions if the background density profile has complex variations rather than decreasing monotonically with altitude. This mechanism predicts that the lowest frequency MFB must exceed the maximum L-cutoff frequency in the ionosphere and the highest frequency MFB must be lower than the maximum plasma frequency. Broughton et al. (2012) use incoherent scatter radar data in combination with MFB observations to confirm these conditions for a large number of cases. In another study, direction of arrival measurements of MFB combined with ray-tracing calculations indicate that MFB often originates near 200 km altitude in the topside of a disturbed ionosphere under intense auroral arcs in which the peak electron density occurs in the E-region (Burnett and LaBelle, 2020). (Broughton et al., (2012) also shows that MFB is associated with ionospheric profiles having peak density in the E-region).

Alternative mechanisms have been suggested for MFB, such as mode conversion of electron acoustic and electron cyclotron harmonic waves generated by gyrating electron beams (Sotnikov et al., 1995). Since these wave modes are fundamentally broadband, generation would be at a single location not over a range of altitudes as was the case for the Langmuir wave mechanism. The condition for excitation in the frequency range of MFB is that f_{pe} be at least a few times f_{ce} as could occur in the enhanced density under the expanding substorm arc. The electrostatic waves excited near the peak density would extend down to the electron cyclotron frequency or even below in the case of electron acoustic waves. In this scenario mode-converted waves have access to the ground since they are generated below the peak in the L-cutoff frequency. Bunch et al. (2009) show that excitation of these electrostatic modes by auroral electron distributions is possible, though there is no natural condition for linear conversion to the LO-mode, and for the assumed distribution functions the growth rate was favorable for frequencies near or slightly above f_{ce} relevant to "low band" MFB but not "high band" MFB. Another generation mechanism put forth for MFB is excitation in strong Langmuir turbulence "cavitons." Akbari et al. (2013) found several instances of temporal correlation between MFB and strong Langmuir turbulence measured with the PFISR radar. Hudson et al. (2022) in a statistical study of more than 100 MFB events coincident with PFISR radar observations showed these instances to be rare but could neither prove nor disprove that the phenomena might be correlated.

MFB is the least understood of the auroral emissions types. Basic parameters such as source altitude and extent are unknown. These parameters are critical to determining which, if any, of several proposed generation mechanisms applies. Ground-level direction-finding data combined with ray tracing calculations suggest relatively low source altitudes (Burnett and LaBelle, 2020),

in conflict with model calculations based on generation from mode-converted Langmuir waves (LaBelle, 2011), rocket observations showing Langmuir waves generally more prevalent in the auroral zone above 600 km (though they also occur at lower altitudes), and interpretation of the ~3-MHz null in the MFB spectrum as cyclotron absorption near 300-km altitude. Source height estimates are challenging using ground-based data alone because of difficulty assessing ionospheric refraction and absorption in the disturbed auroral ionosphere. If possible, satellite-based direction-finding observations of MFB would avoid these difficulties. Definitive determination of MFB source heights and sizes is an essential priority for identifying the generation mechanism.

Observation of electromagnetic radiation from auroral Langmuir waves and identifying conditions and mechanisms of such radiation are key questions relevant to MFB. There is strong evidence for whistler mode radiation from auroral Langmuir waves when $f_{pe} < f_{ce}$ (Beghin et al., 1989; McAdams and LaBelle, 1999). MFB requires radiation into LO-mode when $f_{pe} > f_{ce}$ (LaBelle, 2011). Under these conditions, rockets observe structured waves at and just above f_{pe}, sometimes discretized through trapping in small-scale density irregularities and sometimes propagating into lower densities (Beghin et al., 1989; McAdams and LaBelle, 1999; McAdams et al., 2000). However, rocket observations have not been sufficiently sensitive to detect LO-radiation streaming away from these, with the possible exception of second harmonic emission reported by Boehm. (1987). Assuming such radiation exists, an open question is whether the mechanism responsible is linear or nonlinear mode conversion. Confirmation of occurrence of either mechanism from *in situ* measurements in the auroral ionosphere would be important evidence relevant to MFB.

An important characteristic of MFB is its association with substorm onset. The prompt onset of MFB simultaneous with other signatures such as auroral brightening points to its possible application to pin down the timeline of solar wind-magnetosphere-ionosphere coupling. Ground-level MFB often occurs simultaneous with and comes from the direction of the initial poleward-expanding substorm arc, but ground level observations cease shortly after onset due to absorption caused by enhanced ionization. Therefore, ground-level observations cannot exclude that the emission might also originate in arcs other than the initial poleward-expanding one, or whether the emission continues past the initial onset phase into the recovery phase. Satellite detections, immune from effects of ionospheric propagation, could definitively answer these questions, which have implications for remote sensing using MFB. Such observations would also pin down the intensity of the emissions, without uncertainties due to ionospheric propagation and absorption which affect the ground-level measurements.

Propagation and scattering of MFB signals, as well as how and where they reach ground-level, are key questions for understanding the phenomenon, interpreting the ground-level observations, and developing remote sensing techniques. If linear mode-conversion of Langmuir waves generated by parallel electron beams causes MFB, the initial direction of the mode-converted waves should be mostly downward, and scattering from the enhanced density below the source or from density irregularities would be responsible for observation over a range of distances at ground level. Bunch et al. (2009) show examples in which higher frequency MFB arrives from higher elevation angles than lower frequency MFB. This could arise if the MFB comes from sources matching the plasma frequency on the bottomside, but it could also be consistent with generation through linear mode conversion of topside Langmuir waves initially vertically downward propagating and scattered by the underlying high-density ionosphere. In this latter case, satellite observations above the source would only be possible because of scattering or reflection from the dense plasma beneath the source, though satellites or rockets flying under the source could observe the direct emission. If the mode-conversion is nonlinear, a wide range of initial EM wave directions is possible allowing direct illumination of receivers both above and below the sources. Ground-based direction-finding observations provide important clues, but direction-finding or radio imaging from satellites would provide a more effective means to distinguish these mechanisms. Simultaneous ground-based and satellite imaging would not only test these source mechanisms but would also enable assessment of the impact of ionospheric propagation and absorption on the ground-level observations.

As with cyclotron harmonic radiation, an outstanding question concerning MFB is explaining the wide range of fine frequency- and temporal-structure that characterizes the phenomenon. In the case of MFB, the range of frequency-time patterns is truly astounding, including upward-going, downward-going, up-and-down, and monochromatic features. A common feature is a descending frequency tone called the "backward seven" (Bunch and LaBelle, 2009), which with some assumptions can be explained by mode-conversion of Langmuir waves by relatively low energy precipitating electrons on the downward-pointing density gradient in the topside ionosphere (LaBelle, 2011). Qualitatively, this mechanism can explain other shapes of fine structures by assuming a other variations of density with altitude, although this has not been investigated quantitatively. There is some evidence that ascending frequency tones are more common at the lowest MFB frequencies, presumably near the L-cutoff. It remains uncertain whether suggested MFB mechanisms explain any, let alone all, of the wide variety of MFB fine structures. Multiple mechanisms may play a role in creating these.

Also similar to auroral cyclotron harmonic emissions, MFB shows promise for remote sensing of ionospheric density and density structure. If MFB represents radiation from Langmuir waves, the observed frequency corresponds to plasma density at the source altitude. A combination of wave dispersion and ray-tracing, with some reasonable assumptions, then allows the observed MFB frequency dispersion to be inverted to determine a portion of the density profile (e.g., LaBelle, 2011). If MFB comes from Alfvénic arcs at substorm onset, the profile would correspond to those interesting and significant field lines containing the precipitating electrons. Another open question is whether MFB is a remote indicator of nonlinear Langmuir turbulence, as suggested by a few case studies (Akbari et al., 2013). Ground-based observations reported by Hudson et al. (2022) do not provide a definitive answer to this question.

4 LF-MF auroral hiss emissions

VLF auroral hiss has been widely studied (e.g., Makita, 1979; Sazhin et al., 1993), but LF-MF auroral hiss has received less

attention, although it has also been observed for a long time (e.g., Jorgensen, 1969; Laaspere et al., 1971). VLF auroral hiss is broadly divided into two types, continuous and impulsive, and LF-MF hiss has generally been assumed to be an extension of the impulsive type (e.g., Laaspere et al., 1971; Morgan, 1977; LaBelle et al., 1994). Although much LF-MF hiss is directly correlated with VLF impulsive hiss and similarly occurs at substorm onsets or other auroral activations, there is a substantial subset, called "LF cutoff" hiss, for which there is no VLF component (LaBelle et al., 1998). (Morgan. (1977) also notes occurrences of LF hiss without a VLF counterpart.) LaBelle et al. (1998) posit a common source for the VLF and LF-MF hiss but attribute "LF cutoff" hiss to propagation effects whereby LF hiss gets through the Earth-ionosphere boundary over a wider range of latitudes than VLF hiss, an effect also suggested by ray-tracing studies of Horne. (1995). It is also possible that "LF-cutoff" hiss results from different generation mechanisms discussed below. Ye and LaBelle. (2008) show that LF-MF hiss takes on a variety of forms, including diffuse-type emission and discrete features, another hint that not all LF-MF hiss is simply an extension of VLF hiss and that other generation mechanisms exclusive to LF-MF may play a role. (Some discrete-type hiss may represent leaked AKR overlapping with hiss.) Another form of structured hiss is "flickering LF auroral hiss," 10–200 Hz fluctuations in intensity with dispersive features suggesting generation near 2,500 km altitude (LaBelle, 2021, and references therein). Figure 3 shows examples of auroral hiss observed at South Pole at frequencies ranging from VLF to MF.

LF-MF whistler mode signals have been observed with suitably instrumented satellites at high latitudes, going back to the ISIS topside sounders (Benson and Wong, 1987) and the EXOS-C wave receivers (Oya et al., 1985; Morioka et al., 1988). Rocket-borne instruments have measured LF-MF whistler mode on both the nightside and the dayside (e.g., Morioka et al., 1988). Featureless impulsive emissions are common, similar to the ground-level observations, but a host of structured emissions occur ranging from banded structures originating as Langmuir wave bursts (Beghin et al., 1989; McAdams and LaBelle, 1999), to whistler-mode stripes at 200–600 kHz (Samara and LaBelle, 2006; Colpitts et al., 2010), to "hook" and "swisher" features (Colpitts et al., 2009). Since most of these features are not observed at ground-level, they may have oblique wave-normal angles that prevent their propagation through the Earth-ionosphere boundary.

Recent examination of 3 months of South Pole data, November 2022-January 2023, reveals approximately 842 min of hiss during 93 days of observation implying an overall occurrence rate of 0.6%, several times higher during the most favorable magnetic local time sector. Yan et al. (2013) report 1111 hiss events across approximately 750 days of observations; assuming approximately 5 min per event yields a similar occurrence rate. (VLF auroral hiss may have considerably higher occurrence rates; for example, Spasojevic. (2016) reports VLF hiss observed during 10% of nighttime 15-min synoptic intervals at South Pole.) The radiance at LF is generally lower than that at VLF. Makita. (1979) reports ground-level measurements to above 100 kHz (their Figure 25), and extrapolating to 300 kHz suggests radiance of 10^{-18} W/m^{2}Hz. LaBelle. (2021) estimates peak radiance approaching 10^{-17} W/m^{2}Hz over the 0–500 kHz range. Benson et al. (1988) show typical field strengths at 150–700 kHz corresponding to about 5×10^{-18} W/m^{2}Hz similar to the above, whereas Benson and Desch (1991) observe field

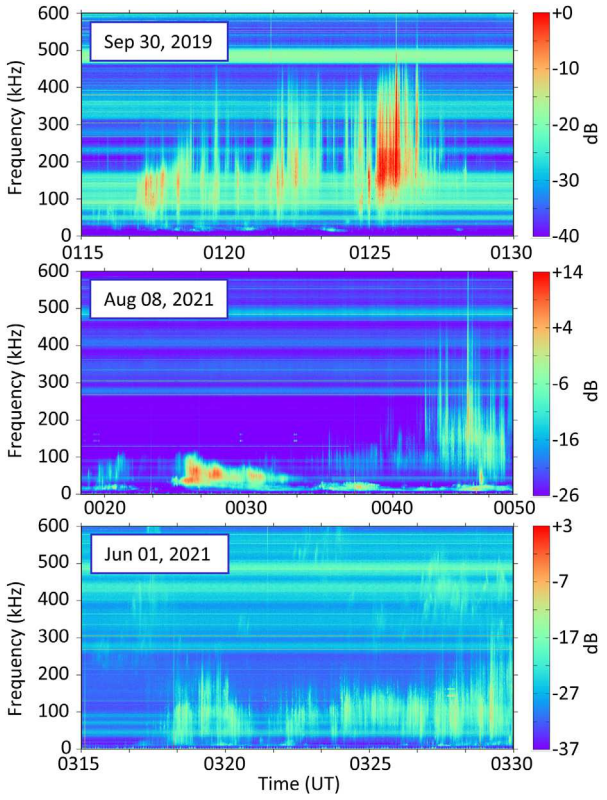

FIGURE 3
Auroral hiss observed with a 40-m^2 loop antenna and digital receiving system at South Pole Station (geomagnetic latitude 74.5°), illustrating impulsive and diffuse LF hiss. Occasional VLF hiss appears despite the instrumental ~100 kHz high-pass filter. The bottom panel shows intermittent AKR above 200 kHz and some discrete features imbedded in the LF hiss.

strengths about 50% higher at 150 kHz. [Ground based observations show stronger hiss intensities at VLF, where radiance may be 10^{-17} to 10^{-15} W/m^{2}Hz at 10 kHz (e.g., Jorgensen, 1968)]. Considerably higher amplitudes are observed in space. Typical radiances observed with the OGO-6 satellite at around 1,000 km are 6×10^{-17} (1.7×10^{-18}) W/m^{2}Hz at 200 (540) kHz, although values up to 5.5×10^{-14} (1.7×10^{-15}) W/m^{2}Hz were observed on occasion (Laaspere et al., 1971). Simultaneous ground-level and space-based measurements of LF/MF hiss have not been done, but the few such studies at VLF suggest that hiss is much more prevalent in the ionosphere than at ground level (e.g., Gurnett, 1966; Srivastava, 1974). Higher radiance and occurrence rates in space are expected because the hiss wave normal vector must lie within a few degrees of vertical in order to penetrate the Earth-ionosphere boundary, whereas hiss in space presumably occupies a wide range of wave-normal angles.

A mechanism for VLF hiss which applies also to LF-MF hiss is coherent amplification by auroral electron beams of whistler mode noise generated through Cherenkov process also from electron beams (Maggs, 1976). Sonwalkar and Harikumar. (2000) point out that for auroral electron beam energies, whistler modes produced by this mechanism must be scattered, in the VLF case by meter-scale ionospheric irregularities, in order to penetrate

the Earth-ionosphere boundary and be observed on the ground. While this mechanism probably explains the bulk of VLF hiss and much LF-MF hiss, other mechanisms may play a role at LF-MF. Two scenarios involving cyclotron maser instability have been investigated. Wu et al. (1983) found that for cold background electron densities higher than the beam density, the instability can excite whistler mode directly in the altitude range 1,500–3,000 km below the acceleration region, with convective growth comparable to the convective beam amplification mechanism. Growth is for frequencies above $f_{ce}/2$ so LF rather than VLF hiss would be generated by this mechanism at these altitudes. Wu et al. (1989) looked at the converse condition of large beam density, predicting Z-mode excitation at near parallel wavenumbers with growth rate peak around $0.8f_{ce}$; the corresponding convective growth would be relatively broadband at LF-MF frequencies as modeled by Ziebell et al. (1991) and could convert to whistler mode and penetrate the Earth-ionosphere boundary to be observed at ground level over a range of latitudes as modeled by Horne. (1995). This mechanism is an alternative to propagation effects as an explanation for LF-cutoff hiss.

An outstanding problem related to auroral hiss, as highlighted by Sonwalkar and Harikumar. (2000), is its penetration to ground level. Whistler waves originating through resonance with auroral electrons are oblique, yet the wave vectors must be vertical in order to penetrate the Earth-ionosphere boundary. Sonwalkar and Harikumar. (2000) find that refraction on reasonable expected ionospheric density gradients is insufficient and propose scattering from density irregularities, meter-scale in the case of VLF hiss, as a mechanism for converting some fraction of the oblique hiss into waves that can reach ground level. The experimental evidence in the ionosphere is somewhat meager, for example, a very early study indicating correlation between hiss occurrence and radar backscatter (Hower and Gluth, 1965). *In situ* measurements of the wave normal angle distribution, as would be possible from fully-sampled waveform measurements of all three components of wave electric field with sufficient sensitivity, would potentially reveal much about the scattering process if it occurs. Direction finding measurements of hiss from space or ground in combination with radar detection of irregularities could also test the theory, although the scattering might in many cases happen at altitudes inaccessible to radar. Theory and modelling of possible scattering processes and subsequent propagation could inform experimental tests of the mechanism. Relevant simulations at VLF have been reported by Lebed et al. (2019).

As with the other emissions, an outstanding question is how different types of LF/MF auroral hiss come about. For example, can the diffuse/patchy type result from the same mechanism as the standard impulsive hiss, but affected by wave propagation and dispersion, or does it require a completely different generation mechanism? Modelling of wave propagation plays a key role in answering this question, but observations of the diffuse/patchy signature in space would provide important clues. Another open question is whether "LF cutoff hiss," lacking a VLF component, results from propagation effects as proposed by LaBelle et al. (1998) or from generation exclusively over an LF band of frequencies, as predicted for cyclotron maser amplification of quasi-parallel Z-mode waves followed by mode conversion (Wu et al., 1989; Ziebell et al., 1991; Horne, 1995). A large set of *in situ* observations spanning VLF to MF could answer this question, since the former mechanism predicts that the "LF cutoff" phenomenon may not occur above the ionosphere, whereas the alternative mechanism predicts the opposite. Discrete features sometimes observed in LF/MF hiss raise the question of whether these are identical to leaked AKR originating at high altitudes or result from ionospheric generation mechanisms or scattering processes as suggested by Ye et al. (2007). Further studies of their morphology and occurrence statistics, either from space or ground-level, might link or distinguish them from leaked AKR. *In situ* observations would test the mechanisms put forward by Ye et al., (2007) by, for example, associating them with Langmuir wave "hot spots" or revealing aspects of wave scattering through wave normal distribution measurements. Another interesting aspect of auroral hiss structure is flickering auroral hiss (LaBelle, 2021, and references therein). If related to flickering aurora, an outstanding question is why it is so rarely observed. Narrow-beam or wave imaging measurements would confirm whether the rarity of flickering hiss is a limitation of the previous observation methods which used broad-beam antennas, whereas flickering aurora is known to come from small patches in the sky. More examples obtained this way would determine the distribution of dispersions of the flickering elements critical to testing whether they originate from modulated Alfvénically accelerated electron beams, a mechanism explaining flickering aurora put forth by Temerin et al. (1986); Temerin et al. (1993) and extended and supported by many subsequent studies (e.g., Sakanoi et al., 2005; Whiter et al., 2010; Fukuda et al., 2017). If flickering aurora and hiss can be observed together, the phase/timing relation between the modulations would provide another effective test of the theory.

A significant aspect of auroral hiss is its connection to storms, substorms, current systems, and other macroscopic space physics processes. Early satellite observations showed an association of LF/MF hiss with upward current region (e.g., Kisabeth and Rostoker, 1979). Furthermore, there is a close association between LF/MF hiss and substorm onsets, as is the case with impulsive VLF hiss (Makita, 1979). However, not all LF/MF hiss occurs at substorm onsets; similar to MFB, LF/MF hiss must often be associated with auroral activity that falls short of substorm onset, or activity preceding and following onset. Furthermore, on occasions LF/MF hiss lasts for time periods of an hour or more which is uncharacteristic of substorm onset. LF/MF hiss is clearly generated under a range of auroral conditions. Dayside LF/MF hiss presents a different mystery: Yan et al. (2013) show that detection of pre-noon MLT auroral hiss at South Pole Station depends on IMF By and put forth that under conditions of negative By the resulting shift of field-aligned currents puts the upward currents become dominant at South Pole latitudes in the pre-noon sector. This theory would predict an opposite IMF By dependence in the northern hemisphere, but preliminary studies of dayside hiss occurrence at Sondrestrom, at nearly the same magnetic latitude as South Pole, show no IMF By preference of the occurrence rate of dayside LF/MF hiss. The relationship of LF/MF hiss to auroral current systems is an open area of study (Spasojevic. (2016) has shown some interesting correlations between VLF hiss occurrence and current systems.). Ground-level measurements of auroral hiss (and MFB) complement spacecraft missions such as AMPERE and Swarm which give global and local views of the field-aligned current systems.

The above considerations highlight possibilities to develop remote sensing of auroral current systems or substorm activity using LF/MF auroral hiss. One application is timing and location of substorm onsets associated with hiss, which would allow confirmation of inter-hemispheric asymmetries in latitude and magnetic local time through conjugate observations of auroral hiss. As discussed above, the dispersion of elements of flickering auroral hiss potentially provides information about Alfvénically accelerated electrons and their characteristics. Despite previous modelling and theory (e.g., Maggs and Lotko, 1981), it is still not fully understood or experimentally confirmed what controls the frequency range of LF/MF hiss, which can vary dramatically by over a factor of ten (from <100 kHz to well over 1 MHz). Presumably the altitude of emission is an important factor since generation in the whistler mode requires $f < f_{ce}$. Remote sensing of auroral beam fluxes and energies could result from a better understanding of observable properties of LF/MF auroral hiss.

5 Leaked auroral kilometric radiation

Auroral Kilometric Radiation (AKR) usually refers to LF/MF radio waves generated by auroral electrons via the cyclotron maser instability; when operating on the "horseshoe" rather than pure loss-cone electron distribution in the low density auroral acceleration region where $f_{pe}/f_{ce}<<1$, this mechanism can be extremely efficient, converting up to ~1% of the auroral energy into radio waves (Pritchett et al., 1999; reviews by Ergun et al., 2000; Treumann, 2006). The component of this radiation which is primarily X-mode and directed away from the Earth, called "escaping AKR," was detected by spacecraft in the 1960s (Benedictov et al., 1966; Dunkel et al., 1970) but first described and recognized as significant by Gurnett (1974) and subject of many recent reviews (e.g., Baumjohann and Treumann, 2022) and current studies on processes driving structuring of the emissions (e.g., Pottelette and Berthomier, 2017) as well as their connection to substorm activity (e.g., Waters et al., 2022; Fogg et al., 2022). It was originally thought that AKR consisted exclusively of this escaping component, explaining why its discovery depended on deployment of suitably instrumented spacecraft. However, as early as the late 1970's reports appeared of AKR-like radio emissions observed in the lower ionosphere, called "leaked AKR" (Oya et al., 1979). The low-Earth orbit EXOS-C satellite detected many examples (Oya et al., 1985), as did the APEX spacecraft (Shutte et al., 1997). Suitably instrumented sounding rockets picked up structured whistler mode waves at 200–600 kHz resembling AKR but at ionospheric altitudes (Morioka et al., 1988; LaBelle et al., 1999). Recently, the low-Earth-orbiting spacecraft DEMETER reported observations of leaked AKR, initially from a storm-time interval which shifted the auroral oval to latitudes probed by the satellite (Parrot and Berthelier, 2012), and subsequently from the entire mission, showing evidence for a possible hemispheric asymmetry (Parrot et al., 2022). Leaked AKR has also been observed at ground level (e.g., Figure 3 of LaBelle et al., 1999). Several years of observations at South Pole Station and Antarctic Automated Geophysical Observatories (AGO's) have measured hundreds of events (LaBelle and Anderson, 2011; LaBelle et al., 2015; LaBelle et al., 2022; LaBelle and Schwartz, 2023). Figure 4 shows South Pole measurements of leaked AKR exhibiting frequency and time variations characterizing these emissions and distinguishing them from LF/MF auroral hiss.

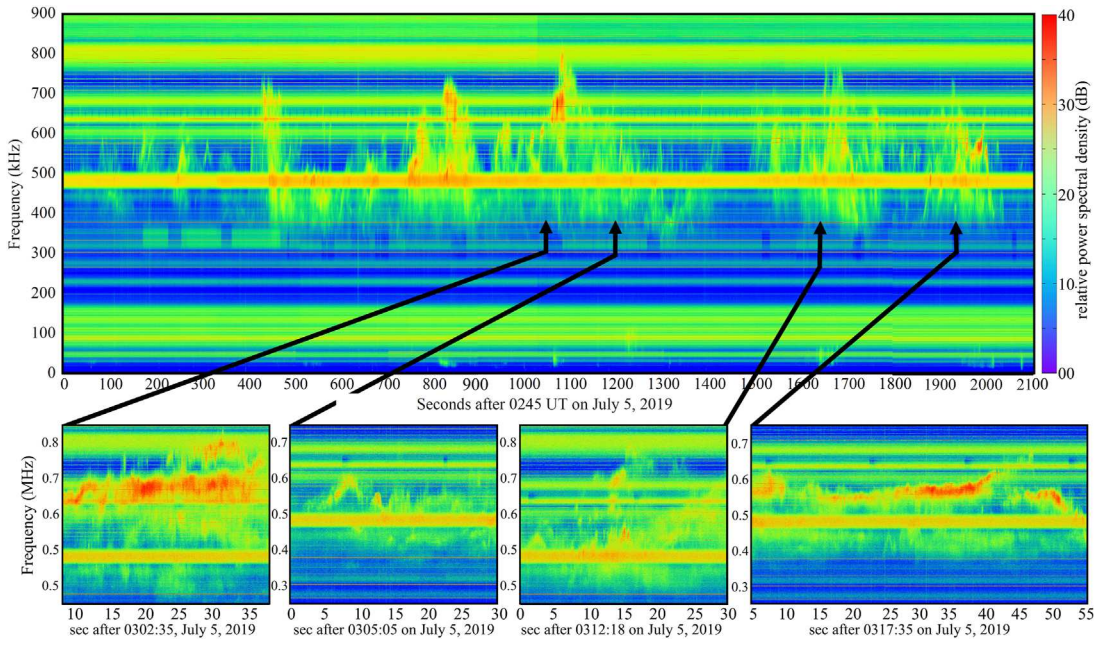

FIGURE 4
Leaked AKR observed at South Pole Station, Antarctica, on 5 July 2019. The bottom panels show expanded plots of the fine structure. The instrumentation used for these measurements is identical to that used for those shown in Figure 3. Horizontal lines result from radio frequency interference and should be ignored.

The leaked AKR occurrence rate at ground level can be estimated from the approximately 1,000 min/year of observations at South Pole in 2018–2020 concentrated in an approximately 90-day interval each year and a 5-h interval around magnetic midnight each day, implying 3.7% occurrence rate during favorable season and magnetic local time (LaBelle and Schwartz, 2023). In low-Earth orbit, the phenomenon was observed in more than 2% of the DEMETER passes above the auroral zones (Parrot et al., 2022); this value may be an underestimate because DEMETER probed primarily sub-auroral latitudes during the declining phase of the unusual solar cycle 23 which had an extended minimum. Ground-level AKR events typically have maximum radiance in the range 10^{-18} to 10^{-17} W/m^{2}Hz, with a tail of events extending to 10^{-16} W/m^{2}Hz. Many weaker events may lie below instrument detection threshold. Higher intensities have been observed in space. Examples measured by sounding rocket had estimated radiance of up to a few times 10^{-14} W/m^{2}Hz (LaBelle et al., 1999). Power spectral densities observed with the DEMETER satellite range 0.03–25 μV^2/m^{2}Hz (Parrot et al., 2022), corresponding to 6×10^{-16} to 6×10^{-14} W/m^{2}Hz assuming free space propagation. For reference, escaping X-mode AKR has larger or comparable radiance at large distances from the sources, for example, 10^{-14} at 25 R_E in Figure 3 of Gurnett. (1974).

From the time of its discovery, leaked AKR attracted attention to its possible generation mechanisms. These fall into roughly two categories: emission in the acceleration region close to the sources of escaping AKR, and emission at lower altitudes. Krasovskiy et al., 1983 proposed ballistic wave transformation in which AKR generation in the auroral acceleration region imprints the electron distribution which then re-radiates an echo of the AKR in the whistler mode at lower altitudes. Scaling arguments suggest that this mechanism could be more efficient than mode-conversion mechanisms. Chian et al. (1994) suggest that radiation in the AKR frequency range could result from nonlinear interaction of Langmuir and Alfvén waves. Wu et al. (1983), Wu et al. (1989) consider excitation of parallel propagating Z-mode waves via the maser instability, finding an instability that peaks at $f \sim 0.8 f_{ce}$, in contrast to the maser production of perpendicular X-mode responsible for escaping AKR, which peaks at $f \sim f_{ce}$. By this mechanism combined with conversion to whistler-mode, a particular frequency of leaked AKR would be produced perhaps ~1,000 km lower on the field line than the sources of escaping AKR of the same frequency. Propagation to ground level is possible as shown by Horne. (1995). However, this mechanism predicts broadband radiation, as confirmed by calculations of Ziebell et al. (1991), which fits better to certain types of LF auroral hiss, which is broadband, rather than leaked AKR which consists of multiple narrowband fine structures (LaBelle et al., 2015; LaBelle et al., 2022).

The other class of explanations of leaked AKR involve sources in close proximity to those of escaping AKR. Oya et al. (1985) put forth that Z-mode waves could be produced in the close vicinity of the acceleration region, as proposed by Oya and Morioka. (1983) as part of an explanation for the small component of O-mode observed in escaping AKR. The direct connection between the Z- and whistler modes where the Z-mode frequency matches the local plasma frequency enables an efficient mode conversion (Jones, 1976), and the resulting whistler modes could propagate to low altitude as leaked AKR. Morioka et al. (1988) state that the relevant mode conversion rate would be more than 1%, though they argue for an inverse Landau interaction rather than cyclotron maser instability as responsible for the original Z-mode waves. More recently, Mutel et al. (2011) shows direct evidence for the existence of Z-mode waves in the auroral acceleration region in close proximity to escaping X-mode AKR sources: when the Cluster satellites traverse near those sources, its wave instruments detect a null in the radio spectrum which varies in a characteristic manner resulting from the forbidden region in the dispersion surfaces of the Z- and X-modes. Mutel et al. (2011) complement the observations with calculations of cyclotron maser growth rates of perpendicular modes in conditions of the auroral acceleration region: X-mode is excited under the lowest density conditions ($f_{pe} << f_{ce}$) in the central regions of the auroral acceleration region, and Z-mode is excited in regions where f_{pe}/f_{ce} is not quite as low; at given locations, X-mode can be excited at higher frequencies and Z-mode at lower frequencies with a narrow gap in between. (In both cases the excited frequencies are in a narrow frequency range just below local f_{ce}.) These observations and calculations allow refinement of the original idea proposed by Oya et al. (1985), suggesting that indeed Z-mode is generated in the auroral acceleration region in close proximity or even coinciding with sources of escaping X-mode radiation, but the excited modes are perpendicular and hence must either refract to parallel to undergo linear conversion to whistler mode or alternatively undergo nonlinear conversion on strong density gradients or in the presence of strong density irregularities. The resulting whistler mode waves propagating to low altitudes would be observed as leaked AKR. This mechanism suggests a close connection between leaked and escaping AKR.

The outstanding problem concerning leaked AKR is to determine its source location and mechanism and hence its degree of connection to the primarily X-mode escaping AKR which has been the object of intensive study for decades. A connection between leaked and escaping AKR is suggested by examples of leaked AKR observed at South Pole Station, Antarctica, coincident and somewhat correlated with bursts of escaping AKR measured with the Geotail spacecraft more than 10^5 km away (LaBelle and Anderson, 2011). LaBelle et al. (2015) expanded this study, showing many more partly-correlated events and statistical correlations at the 2-3σ confidence level between ground-level leaked AKR and escaping AKR measured with Geotail. They also show simultaneous detections of leaked AKR at up to four Antarctic observatories, suggesting that the area illuminated by the phenomenon can be as large as ~10^6 km^2, either through direct illumination by high altitude sources or through sub-ionospheric propagation of ducted or concentrated radiation. The polarization is consistent with whistler mode propagation in the ionosphere. Proving a direct connection between escaping and leaked AKR based on statistical correlations alone is challenging, because not all AKR sources illuminate a given satellite or ground station, and particular satellites or ground stations can each detect AKR sources not visible to the other. Therefore, even if the sources of leaked and escaping AKR coincide spatially and temporally, observations of leaked AKR at any particular satellite or ground station would be imperfectly correlated with observations of escaping AKR made with a particular satellite. To meet this challenge, LaBelle et al. (2022) adopted a strategy seeking correlations between the

complex AKR fine frequency structure simultaneously observed in leaked AKR and escaping AKR, for which even a small number of coincidences would comprise "smoking gun" evidence of a direct connection between these phenomena. This initial study employing data from South Pole Station and the Cluster satellites found some intriguing correlations but short of definitive proof. Establishing a direct connection between leaked and escaping AKR would be interesting for several reasons. For example, techniques developed to remotely sense the auroral acceleration region using escaping AKR could be applied to leaked AKR observable at ground level. Other planetary radiations analogous to escaping AKR might be expected to have a corresponding leaked AKR phenomenon.

A key unknown about leaked AKR is the source height; that is, whether it is generated in the auroral acceleration region, thousands of kilometers below, or even in the ionosphere through mode conversion of Langmuir waves as put forth by Ye et al., (2007) to explain discrete features in auroral hiss. If the source is high altitude, a secondary question is whether the waves are ducted to low altitude by field-aligned density structure or propagate in non-ducted mode. If mode conversion is involved, the required efficiency is an open question, as well as whether structure is imparted to the waves by mode-conversion or in scattering processes. These questions are difficult to answer with ground-based observations alone because of the roles of ionospheric absorption, penetration through the Earth-ionosphere boundary, and sub-ionospheric propagation, but they could be answered with a satellite with continuous direction-finding or imaging ability flying under or through the sources.

Ground-based (South Pole) and satellite (DEMETER) observations raise a number of interesting issues. DEMETER observations suggest a strong hemispheric asymmetry with occurrence rate over 30% larger in the northern hemisphere than in the south, a difference that decreases for higher auroral activity (Parrot et al., 2022). In contrast, ground-level observations are almost exclusively from the southern hemisphere, where hundreds of events have been reported *versus* just a single event documented in the northern hemisphere, an effect attributed to greater radio frequency interference in the northern hemisphere, although that hypothesis has not been investigated quantitatively to confirm whether it is consistent with the extreme difference in the observations. Escaping AKR shows a weak tendency for favoring northern hemisphere as well (Mutel et al., 2004). Another issue raised by observations concerns the frequency range of leaked AKR. Ground-level observations show a frequency distribution concentrated at 400–600 kHz, at the high end of the range of frequencies observed in escaping AKR (LaBelle et al., 2015; LaBelle and Schwartz, 2023). If generation is at local f_{ce} as for escaping AKR, this would put the sources at the low end of the range of sources that illuminate outer space, and it might be reasonable that lower altitude sources have a better chance of exceeding a detection threshold at low altitudes. On the other hand, DEMETER satellite observations suggest the range of frequencies at low Earth orbit is comparable to that of escaping AKR (Figure 12 of Parrot et al., 2022). This suggests that the discrepancy might be due to frequency-dependent differences in ability of the waves to penetrate the Earth-ionosphere boundary, perhaps from variations in wave-normal angle distribution due to propagation or source-height effects. The two order of magnitude difference in the intensity of ground-based *versus* spacecraft-based observations suggests that the bulk of leaked AKR does not penetrate the Earth-ionosphere boundary. *In situ* observations of the wave normal angle distribution of leaked AKR as a function of frequency would shed light on these discrepancies.

Another outstanding question about leaked AKR is finding explanations for the wide range of fine structure characteristics it

LF/MF/HF auroral radio emissions observable at ground level

type	frequency	polarization	outstanding problems
Auroral Hiss	<1.2 MHz (below f_{ce})	Right (W-mode)	Mechanism of penetration to ground level Sources of different types, source altitudes Connection to substorms, current systems, use for substorm onset timing Dayside hiss
Leaked AKR	200-900 kHz (mostly 400-600 kHz at ground level) (below f_{ce})	Right (W-mode)	Generation mechanism/connection to escaping AKR? Wide range of fine structure Ducted or nonducted propagation/area illuminated? Interhemispheric asymmetry? Remote sensing applications
Cyclotron harmonic emissions	~2.8 MHz ($2f_{ce}$) ~4.1 MHz ($3f_{ce}$) ~5.4 MHz ($4f_{ce}$) ~6.5 MHz ($5f_{ce}$)	Left (subset of $4f_{ce}$ are Right)	Nonlinear generation mechanism of $4f_{ce}$? Wide range of fine structure Connection to flickering aurora Remote sensing applications
Medium Frequency Burst	1.4-5.5 MHz (above f_{ce})	Left (L-mode)	Generation mechanism? Connection to substorms, current systems, use for substorm onset timing? Connected to Langmuir cavitation? Wide range of fine structure, gap at $2f_{ce}$

FIGURE 5
Summary of auroral radio emissions observable at ground level.

displays, similar to escaping AKR. As first reported by Gurnett and Anderson (1981), escaping AKR has complex fine structure. With escaping AKR, convincing interpretations exist for certain types of fine structure, such as "striated AKR" (Menietti et al., 2000; Mutel et al., 2006). Possibly these explanations carry over to similar features observed in leaked AKR, particularly if the two phenomena are closely connected. However, a significant portion of the broad range of fine structure features of both escaping and leaked AKR remain unexplained.

Escaping AKR is an effective probe of the altitude range of the auroral acceleration region, and nearly continuous monitoring possible with the distant Geotail satellite has revealed a number of characteristics of polar substorms revealed through this technique (e.g., Morioka et al., 2007; Morioka et al., 2014, and references therein). Several recent studies have further illuminated connections between escaping AKR and characteristics of substorms (Waters et al., 2022; Fogg et al., 2022). Similarly, certain types of escaping AKR fine structure are indicative of microphysics in the source region (e.g., Mutel et al., 2006). An open question is whether these or other remote sensing techniques can be developed based on ground-based or satellite-based observations of leaked AKR.

6 Conclusion

Figure 5 summarizes the four broad classes of EM radiation from aurora that present a range of challenges to experimenters and theorists. Each is complex and potentially represents multiple phenomena/sub-types. A common element is fine frequency and temporal structure, very little of which is understood, and even when theories exist, confirming experimental evidence is lacking. Another common element is connection to substorm processes, with different types of emissions seeming to relate to different parts of substorms, and some types seemingly related to locations of auroral current regions in ways that are not well understood. A third common element is potential for development of techniques to remotely sense density, temperature, or characteristics of causative electron beams. These problems probably cannot be solved with ground-based data alone, which has limitations due to the roles of auroral absorption, refraction, and conditions for penetration of the waves through the Earth-ionosphere boundary, although great progress could be made with higher resolution direction-finding involving more baselines, wave imaging enabling beam forming or narrow-beam observations, and triangulation from multiple ground-level observatories. Satellite measurements including direction-finding, wave imaging, and determination of wave normal angle distributions could enable breakthrough resolutions of the outstanding problems. Also important are satellite observations of the particle distributions in the source regions in order to determine what instabilities are associated with the auroral emissions. Advances in theory and modelling, including full wave treatments of linear and nonlinear mode conversion and wave propagation, are also essential to understanding the four types of auroral radio emissions. The near-term outlook for all of these techniques looks promising due to technological advances such as cubesat fleets and software defined radio, as well as improvements in high-speed computing.

Author contributions

Sole author JL wrote the manuscript and produced the figures and reference list.

Funding

This work was supported by National Science Foundation grants AGS-1915058 and ANT-2205753 to Dartmouth College with additional support from the AERO project supported by National Aeronautics and Space Administration grant 80NSSC18K1677 in the Heliophysics Technology and Instrumentation Development for Science program.

Acknowledgments

The author wishes to thank many students at Dartmouth College who contributed to this work over the years, as well as the engineers and technicians at Dartmouth, Toolik Lake, and South Pole.

Conflict of interest

The author declares that the research was conducted in the absence of any commercial or financial relationships that could be construed as a potential conflict of interest.

Publisher's note

References

Akbari, H., Semeter, J. L., Nicolls, M. J., Broughton, M., and LaBelle, J. (2013). Localization of auroral Langmuir turbulence in thin layers. *J. Geophys. Res. Space Phys.* 118, 3576–3583. doi:10.1002/jgra.50314

Bale, S. D. (1999). Observation of topside ionosphericMF/HF radio emission from space. *Geophys. Res. Lett.* 26, 667–670. doi:10.1029/1999GL900048

Baumjohann, W., and Treumann, R. A. (2022). Auroral kilometric radiation: the electron cyclotron maser paradigm. *Front. Astron. Space Sci.* 9, 303. doi:10.3389/fspas.2022.1053303

Beghin, C., Rauch, J. L., and Bosqued, J. M. (1989). Electrostatic plasma waves and HF auroral hiss generated at low altitude. *J. Geophys. Res.* 94 (2), 1359–1378. doi:10.1029/JA094iA02p01359

Benediktov, E. A., Getmantsev, G. G., Mitjakov, N. A., Rapoport, V. O., Sazonov, J. A., and Tarasov, A. F. (1966). Intensity measurements of radiation at frequencies 725 and 1525 kc by means of the receiver on the satellite Elektron-2. *Adv. Space Res.* 4, 110.

Benson, R. F., Desch, M. D., Hunsucker, R. D., and Romick, G. J. (1988). Ground-level detection of low- and medium-frequency auroral radio emissions. *J. Geophys. Res.* 93 (1), 277–283. doi:10.1029/JA093iA01p00277

Benson, R. F., and Desch, M. D. (1991). Wideband noise observed at ground level in the auroral region. *Radio Sci.* 26 (4), 943–948. doi:10.1029/91RS00450

Benson, R. F., and Wong, H. K. (1987). Low-altitude ISIS 1 observations of auroral radio emissions and their significance to the cyclotron maser instability. *J. Geophys. Res.* 92 (A2), 1218–1230. doi:10.1029/JA092iA02p01218

Boehm, M. H. (1987). Waves and static electric fields in the auroral acceleration region. Doctoral thesis. Berkeley, CA: Wiley.

Broughton, M. C., LaBelle, J., Kim, E. H., Yoon, P. H., Johnson, J. R., and Cairns, I. H. (2016). On the propagation and mode conversion of auroral medium frequency bursts. *J. Geophys. Res. Space Phys.* 121, 1706–1721. doi:10.1002/2015JA021851

Broughton, M. C., LaBelle, J., and Parrot, M. (2015). DEMETER observations of bursty MF emissions and their relation to ground-level auroral MF burst. *J. Geophys. Res. Space Phys.* 119, 144–155. doi:10.1002/2014JA020410

Broughton, M. C., LaBelle, J., Roberg-Clark, G. T., McCready, M., and Bunch, N. L. (2012). Experimental tests of a topside generation mechanism for auroral medium frequency radio emissions. *J. Geophys. Res.* 117, A12309. doi:10.1029/2012JA018034

Bunch, N. L., and LaBelle, J. (2009). Fully resolved observations of auroral medium frequency burst radio emissions. *Geophys. Res. Lett.* 36, L15104. doi:10.1029/2009GL038513

Bunch, N. L., LaBelle, J., Weatherwax, A. T., and Hughes, J. M. (2008). Auroral medium frequency burst radio emission associated with the 23 March 2007 themis study substorm. *J. Geophys. Res.* 113 (1), 3503. doi:10.1029/2008JA013503

Bunch, N. L., LaBelle, J., Weatherwax, A. T., Hughes, J. M., and Lumerzheim, D. (2009). Experimental tests of the generation mechanism of auroral medium frequency burst radio emissions. *J. Geophys. Res.* 114, A09302. doi:10.1029/2008JA013993

Burnett, A. C., and LaBelle, J. (2020). Estimating polar cap density and medium-frequency burst source heights using 2 f roar radio emissions. *J. Geophys. Res. Space Phys.* 125, e2020JA028166. doi:10.1029/2020JA028166

Carpenter, D. L. (1963). Whistler evidence of a knee in the magnetospheric ionization density profile. *J. Geophys. Res.* 686, 1675–1682. doi:10.1029/jz068i006p01675

Chian, A. C. L., Lopes, S. R., and Alves, M. V. (1994). Generation of auroral whistler mode radiation via nonlinear coupling of Langmuir waves and Alfvén waves. *Astronomy Astrophysics* 290, L13–L16.

Colpitts, C. A., LaBelle, J., Kletzing, C. A., and Yoon, P. H. (2010). Further sounding rocket observations of structured whistler mode auroral emissions. *J. Geophys. Res.* 115, A10243. doi:10.1029/2009JA015095

Colpitts, C. A., Samara, M., LaBelle, J., and Yoon, P. (2009). Rocket observations of two distinct types of dispersive features of auroral HF waves. *J. Geophys. Res.* 114, A05202. doi:10.1029/2008JA013741

Dombrowski, M. P., LaBelle, J., McGaw, D. G., and Broughton, M. C. (2016). An autonomous receiver/digital signal processor applied to ground-based and rocket-borne wave experiments. *J. Geophys. Res. Space Phys.* 121, 7334–7343. doi:10.1002/2016JA022441

Dunckel, N., Ficklin, B., Rorden, L., and Helliwell, R. A. (1970). Low-frequency noise observed in the distant magnetosphere with OGO 1. *J. Geophys. Res.* 75 (10), 1854–1862. doi:10.1029/JA075i010p01854

Ellyett, C. D. (1969). Radio noise of auroral origin. *J. Atmos. Terr. Phys.* 31 (5), 671–682. doi:10.1016/0021-9169(69)90127-5

Ergun, R. E., Carlson, C. W., McFadden, J. P., Delory, G. T., Strangeway, R. J., and Pritchett, P. L. (2000). Electron-cyclotron maser driven by charged-particle acceleration from magnetic field-aligned electric fields. *Astrophysical J.* 538, 456–466. doi:10.1086/309094

Fogg, A. R., Jackman, C. M., Waters, J. E., Bonnin, X., Lamy, L., Cecconi, B., et al. (2022). Wind/WAVES observations of Auroral Kilometric Radiation: automated burst detection and terrestrial solar wind - magnetosphere coupling effects. *J. Geophys. Res. Space Phys.* 127, e2021JA030209. doi:10.1029/2021JA030209

Fukuda, Y., Kataoka, R., Uchida, H. A., Miyoshi, Y., Hampton, D., Shiokawa, K., et al. (2017). First evidence of patchy flickering aurora modulated by multi-ion electromagnetic ion cyclotron waves. *Geophys. Res. Lett.* 44, 3963–3970. doi:10.1002/2017GL072956

Gough, M. P., and Urban, A. (1983). Auroral beam/plasma interaction observed directly. *Planet. Space Sci.* 31 (8), 875–883. doi:10.1016/0032-0633(83)90142-3

Grach, S. M., E N Sergeev, E. N., Mishin, E. V., and Shindin, A. V. (2016). Dynamic properties of ionospheric plasma turbulence driven by high-power high-frequency radiowaves. *Uspekhi Fiz. Nauk.* 59 (11), 1091–1128. doi:10.3367/ufne.2016.07.037868

Gurnett, D. A. (1966). A satellite study of VLF hiss. *J. Geophys. Res.* 71 (23), 5599–5615. doi:10.1029/JZ071i023p05599

Gurnett, D. A., and Anderson, R. R. (1981). "The kilometric radio emission spectrum: relationship to auroral acceleration processes," in *Physics of auroral arc formation, geophysical monograph series*. Editors S. I. Akasofu, and J. R. Kan (Washington DC: American Geophysical Union), 341–350.

Gurnett, D. A. (1974). The Earth as a radio source: terrestrial kilometric radiation. *J. Geophys. Res.* 79 (28), 4227–4238. doi:10.1029/JA079i028p04227

Horne, R. B. (1995). Propagation to the ground at high latitudes of auroral radio noise below the electron gyrofrequency. *J. Geophys. Res.* 100 (8), 14637–14645. doi:10.1029/95ja00633

Hower, G. L., and Gluth, W. I. (1965). Associations between VLF hiss and HF radar echoes from field-aligned ionization. *J. Geophys. Res.* 70, 649–653. doi:10.1029/jz070i003p00649

Hudson, E., LaBelle, J., Reimer, A., and Akbari, H. (2022). A statistical study of auroral medium frequency bursts and anomalous incoherent scatter radar echoes. *Radio Sci.* 57, e2021RS007353. doi:10.1029/2021RS007353

Hughes, J. M., and LaBelle, J. (2001b). First observations of flickering auroral roar. *Geophys. Res. Lett.* 28, 123–126. doi:10.1029/2000gl012210

Hughes, J. M., and LaBelle, J. (2001a). Plasma conditions in auroral roar source regions inferred from radio and radar observations. *J. Geophys. Res.* 106 (10), 21157–21164. doi:10.1029/2001JA000010

Hughes, J. M., and LaBelle, J. (1998). The latitude dependence of auroral roar. *J. Geophys. Res.* 103 (7), 14911–14915. doi:10.1029/98JA01038

Hughes, J. M., LaBelle, J., and Watermann, M. (2001). Statistical and case studies of 2f *ce* auroral roar observed with a medium frequency interferometer. *J. Geophys. Res.* 106 (10), 21147–21155. doi:10.1029/2001JA000009

James, H. G., Hagg, E. L., and Strange, L. P. (1974). "Narrowband radio noise in the topside ionosphere," in *AGARD conference proceedings* (Neuilly sur Seine, France: NATO Advisory Group for Aerospace Research and Development (AGARD)), 24.

Jones, D. (1976). The second Z-propagation window. *Nature* 262, 674–675. doi:10.1038/262674a0

Jorgensen, T. S. (1968). Interpretation of auroral hiss measured on OGO 2 and at Byrd Station in terms of incoherent Cerenkov Radiation. *J. Geophys. Res.* 73 (3), 1055–1069. doi:10.1029/JA073i003p01055

Jorgensen, T. S. (1969). "VLF and LF emissions at auroral latitudes," in *Low-frequency waves and irregularities in the ionosphere, astrophysics and space science library*. Editor N. D'angelo (Dordrecht: Springer). doi:10.1007/978-94-010-3402-9_9

Kaufmann, R. (1980). Electrostatic wave growth: secondary peaks in a measured auroral electron distribution function. *J. Geophys. Res.* 85 (4), 1713. doi:10.1029/JA085iA04p01713

Kellogg, P. J., and Monson, S. J. (1984). Further studies of auroral roar. *Radio Sci.* 19 (2), 551–555. doi:10.1029/RS019i002p00551

Kellogg, P. J., and Monson, S. J. (1979). Radio emissions from the aurora. *Geophys. Res. Lett.* 6 (4), 297–300. doi:10.1029/GL006i004p00297

Kisabeth, J. L., and Rostoker, G. (1979). Relationship of noise in the frequency range $100 < f < 500$ kHz to auroral arcs and field-aligned current and implications regarding acceleration of auroral electrons. *J. Geophys. Res.* 84, 853. doi:10.1029/ja084ia03p00853

Krasovskiy, V. L., Kushnerevskiy, Y. V., Mugulin, V. V., Orayevskiy, V. N., and Pulinets, S. A. (1983). Ballistic wave transformation as a mechanism for the linkage of terrestrial kilometric radio waves with low frequency noise in the upper atmosphere. *Geomagnetism Aeronomy* 23, 702.

Laaspere, T., Johnson, W. C., and Semprebon, L. C. (1971). Observations of auroral hiss, LHR noise, and other phenomena in the frequency range 20 Hz-540 kHz on Ogo 6. *J. Geophys. Res.* 76 (19), 4477–4493. doi:10.1029/JA076i019p04477

LaBelle, J. (2011). An explanation for the fine structure of MF burst emissions. *Geophys. Res. Lett.* 38, L03105. doi:10.1029/2010GL046218

LaBelle, J., and Anderson, R. R. (2011). Ground-level detection of auroral kilometric radiation. *Geophys. Res. Lett.* 38, L04104. doi:10.1029/2010GL046411

LaBelle, J., and Chen, Y. (2016). Right-hand polarized 4f *ce* auroral roar emissions: 1. Observations. *J. Geophys. Res. Space Phys.* 121, 7974–7980. doi:10.1002/2016JA022890

LaBelle, J., and Dundek, M. (2015). Comparison of fine structures of electron cyclotron harmonic emissions in Aurora. *J. Geophys. Res.* 120, 8861–8871. doi:10.1002/2015JA021631

LaBelle, J. (2012). First observations of 5*fce* auroral roars. *Geophys. Res. Lett.* 39, L19106. doi:10.1029/2012GL053551

LaBelle, J. (2021). Flickering low frequency auroral hiss. *J. Geophys. Res. Space Phys.* 126, e2020JA029098. doi:10.1029/2020JA029098

LaBelle, J. (1989). Radio emissions of auroral origin 1968-1988. *J. Atmos. Terr. Phys.* 51 (3), 197–211. doi:10.1016/0021-9169(89)90101-3

LaBelle, J., McAdams, K. L., and Trimpi, M. L. (1999). High frequency and time resolution rocket observations of structured low- and medium-frequency whistler

mode emissions in the auroral ionosphere. *J. Geophys. Res.* 104, 28101–28107. doi:10.1029/1999JA900397

LaBelle, J. (2018). Polarization measurements of unusual cases of medium frequency burst emissions extending below 1.5 MHz. *Earth, Planets Space* 70, 143. doi:10.1186/s40623-018-0912-7

LaBelle, J., and Schwartz, N. (2023). "Statistical characteristics of leaked AKR observed at south pole station, Antarctica," in *Planetary, solar and heliospheric radio emissions IX*. Editors G. Fischer, C. M. Jackman, C. K. Louis, A. H. Sulaiman, and P. Zucca (Dublin: Trinity College Dublin). doi:10.25546/103087

LaBelle, J., Shepherd, S. G., and Trimpi, M. L. (1997). Observations of auroral medium frequency bursts. *J. Geophys. Res.* 102 (10), 22221–22231. doi:10.1029/97JA01905

LaBelle, J., and Treumann, R. A. (2002). Auroral radio emissions, 1. Hisses, roars, and bursts. *Space Sci. Rev.* 101 (3/4), 295–440. doi:10.1023/A:1020850022070

LaBelle, J., Trimpi, M. L., Brittain, R., and Weatherwax, A. T. (1995). Fine structure of auroral roar emissions. *J. Geophys. Res.* 100 (11), 21953–21959. doi:10.1029/95JA01551

LaBelle, J., Weatherwax, A. T., Perring, J., Walsh, E., Trimpi, M. L., and Inan, U. S. (1998). Low-frequency impulsive auroral hiss observations at high geomagnetic latitudes. *J. Geophys. Res.* 103 (9), 20459–20468. doi:10.1029/98JA01562

LaBelle, J., Weatherwax, A. T., Tantiwiwat, M., Jackson, E., and Linder, J. (2005). Statistical studies of auroral MF burst emissions observed at South Pole Station and at multiple sites in northern Canada. *J. Geophy. Res.* 110, A02305. doi:10.1029/2004JA010608

LaBelle, J., Weatherwax, A. T., Trimpi, M. L., Brittain, R., Hunsucker, R. D., and Olson, J. V. (1994). The spectrum of LF/MF/HF radio noise at ground level during substorms. *Geophys. Res. Lett.* 21, 2749–2752. doi:10.1029/94GL02513

LaBelle, J., Yan, X., Broughton, M., Pasternak, S., Dombrowski, M., Anderson, R. R., et al. (2015). Further evidence for a connection between auroral kilometric radiation and ground-level signals measured in Antarctica. *J. Geophys. Res. Space Phys.* 120 (3), 2061–2075. doi:10.1002/2014JA020977

LaBelle, J., Yearby, K., and Pickett, J. S. (2022). South Pole station ground-based and cluster satellite measurements of leaked and escaping auroral kilometric radiation. *J. Geophys. Res. Space Phys.* 127 (2), e2021JA029399. doi:10.1029/2021JA029399

Lebed, O. M., Fedorenkoa, Yu. V., Manninen, J., Kleimenovac, N. G., and Nikitenko, A. S. (2019). Modeling of the auroral hiss propagation from the source region to the ground. *Geomagnetism Aeronomy* 59 (5), 577–586. doi:10.1134/S0016793219050074

Leyser, T. (2001). Stimulated electromagnetic emissions by high-frequency electromagnetic pumping of the ionospheric plasma. *Space Sci. Rev.* 98, 223–328. doi:10.1023/A:1013875603938

Maggs, J. E. (1976). Coherent generation of VLF hiss. *J. Geophy. Res.* 81, 1707–1724. doi:10.1029/JA081i010p01707

Maggs, J. E., and Lotko, W. (1981). Altitude dependent model of the auroral beam and beam-generated electrostatic noise. *J. Geophys. Res.* 86 (5), 3439–3447. doi:10.1029/JA086iA05p03439

Makita, K. (1979). VLF/LF hiss emissions associated with aurora. *Mem. Nat. Ints. Polar Res.* 16, 1–126.

McAdams, K. L., Ergun, R. E., and LaBelle, J. (2000). HF chirps: eigenmode trapping in density depletions. *Geophys. Res. Lett.* 27, 321–324. doi:10.1029/1999gl003655

McAdams, K. L., and LaBelle, J. (1999). Narrowband structure in HF waves above the electron plasma frequency in the auroral ionosphere. *Geophys. Res. Lett.* 26, 1825–1828. doi:10.1029/1999gl900428

Mende, S. B., Carlson, C. W., Frey, H. U., Immel, T. J., and Gerard, J. C. (2003). IMAGE FUV and *in situ* FAST particle observations of substorm aurorae. *J. Geophys. Res.* 108 (4), 8010. doi:10.1029/2002JA009413

Mende, S. B. (2003). FAST and IMAGE-FUV observations of a substorm onset. *J. Geophys. Res.* 108 (9), 1344. doi:10.1029/2002JA009787

Menietti, J. D., Persoon, A. M., Pickett, J. S., and Gurnett, D. A. (2000). Statistical study of auroral kilometric radiation fine structure striations observed by Polar. *J. Geophys. Res.* 105 (8), 18857–18866. doi:10.1029/1999JA000389

Morgan, M. G. (1977). Wide-band observations of lf hiss at Frobisher Bay (L = 14.6). *J. Geophys. Res.* 82 (16), 2377–2386. doi:10.1029/JA082i016p02377

Morioka, A., Miyoshi, Y., Kasaba, Y., Sato, N., Kadokura, A., Misawa, H., et al. (2014). Substorm onset process: ignition of auroral acceleration and related substorm phases. *J. Geophys. Res. Space Phys.* 119, 1044–1059. doi:10.1002/2013JA019442

Morioka, A., Miyoshi, Y., Tsuchiya, F., Misawa, H., Sakanoi, T., Yumoto, K., et al. (2007). Dual structure of auroral acceleration regions at substorm onsets as derived from auroral kilometric radiation spectra: dual structure of acceleration regions. *J. Geophys. Res.* 112, A06245. doi:10.1029/2006JA012186

Morioka, A., Oya, H., Miyaoka, H., Ono, T., Obara, T., Yamagishi, H., et al. (1988). Wave-particle interaction in the auroral ionosphere in LF and HF range: results from antarctic rocket observations. *J. Geomag Geoelectr.* 40, 923–937. doi:10.5636/jgg.40.923

Mutel, R. L., Christopher, I. W., Menietti, J. D., Gurnett, D. A., Pickett, J. S., Masson, A., et al. (2011). "RX and Z-mode growth rates and propagation at cavity boundaries," in *Planetary radio emissions VII*. Editors H. O. Rucker, W. S. Kurth, P. Louarn, and G. Fischer (Vienna: Austrian Academy of Science), 241–252.

Mutel, R. L., Gurnett, D. A., and Christopher, I. W. (2004). Spatial and temporal properties of AKR burst emission derived from Cluster WBD VLBI studies. *Ann. Geophys* 22, 2625–2632. doi:10.5194/angeo-22-2625-2004

Mutel, R. L., Menietti, J. D., Christopher, I. W., Gurnett, D. A., and Cook, J. M. (2006). Striated auroral kilometric radiation emission: a remote tracer of ion solitary structures. *J. Geophys. Res.* 111, A10203. doi:10.1029/2006JA011660

Oya, H., Miyaoka, H., and Miyatake, S. (1979). Observation of HF plasma wave emissions at ionospheric level using sounding rockets S-210JA-1, 2 in Antarctica. *Antarct. Res.* 64, 30–41.

Oya, H., Morioka, A., Koyabashi, K., Izima, M., Ono, T., Miyaoka, H., et al. (1990). Plasma wave observation and sounder experiments (PWS) using the Akebono (EXOS-D) satellite-instrumentation and initial results including discovery of the high altitude equatorial plasma turbulence. *J. Geomag. Geoelectr.* 42, 411–442. doi:10.5636/jgg.42.411

Oya, H., Morioka, A., and Obara, T. (1985). Leaked AKR and terrestrial hectometric radiations discovered by the plasma wave and sounder experiments on the EXOS-C satellite: instrumentation and observation results of plasma wave phenomena. *J. Geomagnetism Geoelectr.* 37, 237–262. doi:10.5636/jgg.37.237

Oya, H., and Morioka, A. (1983). Observational evidence of Z and L-O mode waves as the origin of auroral kilometric radiation from the Jikiken (EXOS-B) satellite. *J. Geophys. Res.* 88 (8), 6189–6203. doi:10.1029/ja088ia08p06189

Parrot, M., and Berthelier, J. J. (2012). AKR-like emissions observed at low altitude by the DEMETER satellite. *J. Geophys. Res.* 117 (10), 17937. doi:10.1029/2012JA017937

Parrot, M., Nemec, F., and Santolik, O. (2022). Properties of AKR-like emissions recorded by the low altitude satellite DEMETER during 6.5 years. *J. Geophys. Res. Space Phys.* 127, e2022JA030495. doi:10.1029/2022JA030495

Pottelette, R., and Berthomier, M. (2017). Nonlinear radiation generation processes in the auroral acceleration region. *Ann. Geophys.* 35, 1241–1248. doi:10.5194/angeo-35-1241-2017

Pritchett, P. L., Strangeway, R. J., Carlson, C. W., Ergun, R. E., McFadden, J. P., and Delory, G. T. (1999). Free energy sources and frequency bandwidth for the auroral kilometric radiation. *J. Geophys. Res.* 104 (5), 10317–10326. doi:10.1029/1998JA900179

Sakanoi, K., Fukunishi, H., and Kasahara, Y. (2005). A possible generation mechanism of temporal and spatial structures of flickering aurora. *J. Geophys. Res.* 110, A03206. doi:10.1029/2004JA010549

Samara, M., LaBelle, J., Kletzing, C. A., and Bounds, S. R. (2004). Rocket observations of structured upper hybrid waves at $f_{uh}=2f_{ce}$. *Geophys. Res. Lett.* 31, L22804. doi:10.1029/2004GL021043

Samara, M., and LaBelle, J. (2006). LF/MF Whistler mode dispersive signals observed with rocket-borne instruments in the auroral downward current region. *J. Geophys. Res.* 111, A09305. doi:10.1029/2005JA011535

Sato, Y., Kadokura, A., Ogawa, Y., Kumamoto, A., and Katoh, Y. (2015). Polarization observations of 4*f ce* auroral roar emissions: polarization of 4fce auroral roar. *Geophys. Res. Lett.* 42, 249–255. doi:10.1002/2014GL062838

Sato, Y., Kumamoto, A., Katoh, Y., Shinbori, A., Kadokura, A., and Ogawa, Y. (2016). Simultaneous ground-and satellite-based observation of MF/HF auroral radio emissions. J. *Geophys. Res. Space Physics*, 121, 4530–4541. doi:10.1002/2015JA022101

Sato, Y., Ono, T., Iizima, M., Kumamoto, A., Sato, N., Kadokura, A., et al. (2008). Auroral radio emission and absorption of medium frequency radio waves observed in Iceland. *Earth Planets Space* 60 (3), 207–217. doi:10.1186/BF03352783

Sato, Y., Ono, T., Sato, N., and Fujii, R. (2010). MF/HF auroral radio emissions emanating from the topside ionosphere. *Geophys. Res. Lett.* 37, L14102. doi:10.1029/2010GL043731

Sato, Y., Ono, T., Sato, N., and Ogawa, Y. (2012). First observations of 4*f ce* auroral roar emissions: fIRST observations of 4*f ce* AURORAL roar. *Geophys. Res. Lett.* 39, L07101. doi:10.1029/2012GL051205

Sazhin, S. S., Bullough, K., and Hayakawa, M. (1993). Auroral hiss: a review. *Planet. Space Sci.* 41, 153–166. doi:10.1016/0032-0633(93)90045-4

Shepherd, S. G., LaBelle, J., and Trimpi, M. L. (1998). Further investigation of auroral roar fine structure. *J. Geophys. Res.* 103 (A2), 2219–2229. doi:10.1029/97ja03171

Shepherd, S. G., LaBelle, J., and Trimpi, M. L. (1997). The polarization of auroral radio emissions. *Geophys. Res. Lett.* 24 (24), 3161–3164. doi:10.1029/97GL03160

Shutte, N., Prutensky, I., Pulinets, S., Klos, Z., and Rothkaehl, H. (1997). The charged-particle fluxes at auroral and polar latitudes and related low-frequency auroral kilometric radiation-type and high-frequency wideband emission. *J. Geophys. Res.* 102, 2105–2114. doi:10.1029/96ja01116

Sonwalkar, V. S., and Harikumar, J. (2000). An explanation of ground observations of auroral hiss: role of density depletions and meter-scale irregularities. *J. Geophys. Res.* 105 (8), 18867–18883. doi:10.1029/1999JA000302

Sonwalkar, V. S. (1995). "Magnetospheric LF-, VLF-, and ELF-waves," in *Handbook of atmospheric electrodynamics* (Boca Raton, Fla: CRC Press).

Sotnikov, V., Schriver, D., Ashour-Abdalla, M., Ernstmeyer, J., and Myers, N. (1995). Excitation of electron acoustic waves by a gyrating electron beam. *J. Geophys. Res.* 100 (10), 19765–19819. doi:10.1029/95JA00900

Spasojevic, M. (2016). Statistics of auroral hiss and relationship to auroral boundaries and upward current regions. *J. Geophys. Res. Space Phys.* 121, 7547–7560. doi:10.1002/2016JA022851

Srivastava, R. N. (1974). Propagation of VLF emissions in the magnetosphere and the ionosphere. *Planet. Space Sci.* 22, 1545–1564. doi:10.1016/0032-0633(74)90019-1

Temerin, M., Carlson, C. W., and McFadden, J. P. (1993). "The acceleration of electrons by electromagnetic ion cyclotron waves," in *Auroral plasma dynamics*. Editors J. Horowitz, N. Singh, and J. Burch (Washington, DC: American Geophysical Union), 155.

Temerin, M., McFadden, J., Boehm, M., Carlson, C. W., and Lotko, W. (1986). Production of flickering aurora and field-aligned electron flux by electromagnetic ion cyclotron waves. *J. Geophys. Res.* 91, 5769–5792. doi:10.1029/JA091iA05p05769

Treumann, R. A. (2006). The electron cyclotron maser for astrophysical application. *Astron. Astrophys. Rev.* 13, 229–315. doi:10.1007/s00159-006-0001-y

Waters, J. E., Jackman, C. M., Whiter, D. K., Forsyth, C., Fogg, A. R., Lamy, L., et al. (2022). A perspective on substorm dynamics using 10 years of auroral kilometric radiation observations from wind. *J. Geophys. Res. Space Phys.* 127, e2022JA030449. doi:10.1029/2022JA030449

Weatherwax, A. T., LaBelle, J., and Trimpi, M. L. (1994). A new type of auroral radio emission observed at medium frequencies (~1350-3700 kHz) using ground-based receivers. *Geophys. Res. Lett.* 21, 2753–2756. doi:10.1029/94GL02512

Weatherwax, A. T., LaBelle, J., Trimpi, M. L., and Brittain, R. (1993). Ground based observations of radio emissions near 2fce and 3fce in the auroral zone. *Geophys. Res. Lett.* 20 (14), 1447–1450. doi:10.1029/GL020i014-p01447

Weatherwax, A. T., Yoon, P. H., Hughes, J. M., LaBelle, J., and Ziebell, L. F. (2006). Further study of flickering auroral roar emission: 2. Theory and numerical calculations. *J. Geophys. Res. Space Phys.* 111 (7), A07302. doi:10.1029/2005JA011288

Whiter, D. K., Lanchester, B. S., Gustavsson, B., Ivchenko, N., and Dahlgren, H. (2010). Using multispectral optical observations to identify the acceleration mechanism responsible for flickering aurora. *J. Geophys. Res.* 115, A12315. doi:10.1029/2010JA015805

Willes, A. J., Bale, S. D., and Kuncic, Z. (1998). A Z-mode electron cyclotron maser model for bottomside ionospheric harmonic radio emissions. *J. Geophys. Res.* 103, 7017–7026. doi:10.1029/97ja03601

Wu, C. S., Dillenburg, D., Ziebell, L. F., and Freund, H. P. (1983). Excitation of whistler waves by reflected auroral electrons. *Planet. Space Sci.* 31 (5), 499–507. doi:10.1016/0032-0633(83)90041-7

Wu, C. S., Yoon, P. H., and Freund, H. P. (1989). A theory of electron cyclotron waves generated along auroral field lines observed by ground facilities. *Geophys. Res. Lett.* 16 (12), 1461–1464. doi:10.1029/gl016i012p01461

Yan, X., LaBelle, J., Haerendel, G., Spasojevic, M., Bunch, N., Golden, D. I., et al. (2013). Dayside auroral hiss observed at South Pole station. *J. Geophys. Res. Space Phys.* 118, 1220–1230. doi:10.1002/jgra.50141

Ye, S., and LaBelle, J. (2008). Ground based observations of low frequency auroral hiss fine structure. *J. Geophys. Res.* 113, A01313. doi:10.1029/2007JA012473

Ye, S., LaBelle, J., and Weatherwax, A. T. (2006). Further study of flickering auroral roar emission: 1. South Pole observations. *J. Geophys. Res.* 111, A07301. doi:10.1029/2005JA011271

Ye, S., LaBelle, J., Yoon, P. H., and Weatherwax, A. T. (2007). Experimental tests of the eigenmode theory of auroral roar fine structure and its application to remote sensing. *J. Geophys. Res.* 112, A12304. doi:10.1029/2007JA012525

Yoon, P. H., LaBelle, J., and Weatherwax, A. T. (2016). Right-hand polarized 4 fce auroral roar emissions: 2. Nonlinear generation theory. *J. Geophys. Res.* 121, 7981–7987. doi:10.1002/2016JA022889

Yoon, P. H., Weatherwax, A. T., and LaBelle, J. (2000). Discrete electrostatic eigenmodes associated with ionospheric density structure: generation of auroral roar fine frequency structure. *J. Geophys. Res.* 105 (12), 27589–27596. doi:10.1029/2000ja000140

Yoon, P. H., Weatherwax, A. T., Rosenberg, T. J., and LaBelle, J. (1996). Lower ionospheric cyclotron maser theory: a possible source of $2fce$ and $3fce$ auroral radio emissions. *J. Geophys. Res.* 101 (12), 27015–27025. doi:10.1029/96JA02664

Yoon, P. H., Weatherwax, A. T., Rosenberg, T. J., LaBelle, J., and Shepherd, S. G. (1998b). Propagation of medium frequency (1-4 MHz) auroral radio waves to the ground via the Z-mode radio window. *J. Geophys. Res.* 103 (12), 29267–29275. doi:10.1029/1998JA900032

Yoon, P. H., Weatherwax, A. T., and Rosenberg, T. J. (1998a). On the generation of auroral radio emissions at harmonics of the lower ionospheric electron cyclotron frequency X, O and Z mode maser calculations. *J. Geophys. Res.* 103 (A3), 4071–4078. doi:10.1029/97JA03526

Yoon, P. H., LaBelle, J., Weatherwax, A. T., and Samara, M. (2006). Mode conversion radiation in the terrestrial ionosphere and magnetosphere, in *Geospace Electromagnetic Waves and Radiation*. Editor J. LaBelle, and R. A. Treumann (Berlin: Springer) 687, 211–234. doi:10.1007/b11580119

Zarka, P. (1998). Auroral radio emissions at the outer planets: observations and theories. *J. Geophys. Res.* 103 (9), 20159–20194. doi:10.1029/98JE01323

Ziebell, L. F., Wu, C. S., and Yoon, P. H. (1991). Kilometric radio waves generated along auroral field lines observed by ground facilities: a theoretical model. *J. Geophys. Res.* 96 (2), 1495–1501. doi:10.1029/>90ja02617